# STATIC AND DYNAMIC BEHAVIOR OF THE LIQUID-VAPOR INTERFACE DURING WEIGHTLESSNESS

by E. W. Otto

NASA Lewis Research Center, Cleveland, Ohio

ABSTRACT

The problems encountered in attempting to operate systems containing a free liquid-vapor interface in a weightless environment are summarized. The literature reporting the research applicable to or directed toward solutions for these problems is reviewed. Results of the research defining the configuration of the interface as a function of liquid properties and system geometry are discussed. The results of experimental studies of the dynamic behavior of the interface in response to changes in gravity level, to outflow disturbances, and to acceleration disturbances are presented. This study places particular emphasis on determination of the scaling laws that permit prediction of the interface behavior as a function of model size.



[redacted]

Presented at the Fluid Dynamics Panel specialists' Meeting, sponsored by the Advisory Group for Aeronautical Research and Development, Marseille, France, April 20-24, 1964

# STATIC AND DYNAMIC BEHAVIOR OF THE LIQUID-VAPOR INTERFACE DURING WEIGHTLESSNESS

by E. W. Otto

Lewis Research Center

E-2545

## 1. INTRODUCTION

The increasing sophistication of space vehicles and their missions has subjected an increasing variety of liquid-vapor systems containing a free interface to a new environment--that of zero gravity. On the Earth these systems rely almost invariably on the body force created by the Earth's gravitational field to separate and locate the liquid and vapor in a consistent predictable manner. Thus, liquids settle to the bottom of tanks, vapors separate from liquids and can be vented off if necessary at the high points in systems, and free convection and buoyancy effects assist in the transfer of heat. In a zero-gravity or weightless environment, however, the gravitational or acceleration body forces are absent, which introduces a number of questions concerning the behavior of the liquid, both static and dynamic, and the effect on heat-transfer phenomena. This paper presents a survey of the various problem areas in the liquid-vapor systems to be used aboard spacecraft and a review of the literature reporting the research applicable to or directed toward the solutions for these problems. The results of experimental studies of the behavior of the interface in response to changes in gravity level, to outflow disturbances, and to acceleration disturbances with particular emphasis on the scaling laws governing the phenomena are also presented.

## 2. PROBLEM AREAS

### 2.1 Propellant Tank Systems

A schematic diagram of a typical space vehicle propellant tank system is shown in Fig. 1(a). Main propellant tanks contain a large, free liquid-vapor interface that is subject to a number of disturbances, such as heat gain and acceleration perturbations, as shown.

The primary function of a propellant tank system is to store the liquid in readiness for use by the engine. Thus the behavior of the interface and the propellant in response to the various disturbances will be important to the engine restart operation. If these perturbations are sufficiently severe, they may move liquid completely away from the area of the pump inlet, thus making it necessary to collect the liquid by acceleration of the vehicle along the thrust axis before attempting to restart the engine. Even if the liquid is over the inlet there is the problem of a limited quantity of liquid being available to the pump due to the possible pull-through of the liquid immediately above the tank outlet and the consequent ingestion of excessive vapor.

The heat gained by the tank may necessitate venting during long storage conditions. The required frequency of venting will depend on the effect of the zero-gravity environment on the heat-transfer mechanism. The success of the venting operation will depend on the behavior of the liquid in response to the disturbances. It may be necessary to collect the liquid and vapor before each vent cycle in the same manner as for the engine starting operation.

The perturbations of the attitude control system, if sufficiently

severe or if in resonance with the natural frequency of the surface, may cause liquid to move over the top of the tank and down the other side. Aside from causing trouble with venting procedures and possibly pumping operations, this liquid circulation constitutes a shifting center of gravity of the vehicle and may cause severe stability problems in the attitude control system.

## 2.2 Space Power Systems

A schematic diagram of a typical space power system is shown in Fig. 1(b). Two free liquid-vapor interfaces normally occur in these systems, one in the evaporator and one in the condenser. The behavior of these interfaces is complicated by the addition of heat in the evaporator, the removal of heat in the condenser, and the probable impact of droplets at high velocity on the interface in the condenser.

The principal fluid dynamic problems in these systems are the avoidance of liquid carryover from the evaporator to the turbine and of vapor carryover from the condenser to the pump inlet. In a normal gravity or equivalent acceleration environment these problems are avoided by proper elevation and orientation of the various components. In a weightless environment where the stabilizing effects of buoyancy are absent, however, liquid and vapor carryover may become difficult to avoid. The situation may be aggrevated by random acceleration from attitude thrustors, drag, crew movements, etc. Further complications will come from the loss of obvious positional stability between tubes of evaporators and condensers employing multiple tubes and from possible changes in heat-transfer mechanisms in the tubes.

## 2.3 Life Support Systems

A schematic diagram of a typical configuration of a life support system employing a subcritical or liquified storage system for the oxygen is shown in Fig. 1(c). Two large, free liquid-vapor interfaces occur in these systems, one in the oxygen supply tank and one in the water receiver tank. A third liquid-vapor interface is found in the water separator.

The problems in the tank systems are similar to those encountered in the main propellant tank except that here the principal problem is to produce or vent vapor from the tank without loss of liquid. In the case of the oxygen supply tank this vapor is generated by the addition of heat, and any changes in heat-transfer mechanisms will become important as in the propellant tank system and in the evaporator of the space power system. In addition, because the heat must be added to the liquid in order to generate vapor, the configuration, location, and dynamic behavior of the liquid will be important in designing the heating system. The acceleration perturbations imposed by attitude thrusters, drag, crew movements, etc. will cause movements of the liquid in each tank similar to that in the main propellant tank.

The separation of water or water vapor from a moving gas stream is usually accomplished by impingement of the air stream against a cooled surface, which condenses the water vapor. The water then drains by gravity to the receiver. In a weightless environment the draining action is lost and other means must be found to remove the water from the condensing surface.

### 2.4 Fuel Cell Systems

Figure 1(d) shows a typical fuel cell system using oxygen and hydrogen, both stored in a liquid state. The problems encountered in this system are the same as those of life support systems.

### 2.5 Miscellaneous Systems

The principal fluid dynamic problems in weightlessness have been illustrated in the previous discussions of the various systems. These problems occur to a greater or lesser extent in all space vehicle systems containing liquid and vapor. There are certain zero-gravity problems, however, that are not fully covered by the previous examples and that have been receiving and will continue to receive a great deal of attention--namely the biomedical problems. Those aspects of the biomedical problem that involve a liquid-vapor interface are subject to the same fluid behavior description as for mechanical systems, although they are probably not subject to the same solutions. Many of the biomedical problems appear, however, to be related to the effect on individual cell behavior of the loss of molecular body forces, which is beyond the scope of this paper.

### 2.6 Summary of Problems

Despite the great variety of systems, the fluid behavior problems can be resolved into a few basic categories as follows:

1. Interface Configuration
    a. Shape and location of the interface
    b. Separation of liquid and vapor
2. Interface Dynamics
3. Pool Boiling Heat-Transfer Mechanisms
4. Evaporation and Condensation Phenomena

It will be found convenient to discuss the fluid behavior phenomena in terms of these broad categories. In the following section a review of the analytical and experimental research studying these phenomena will be made. This is not intended to be an exhaustive review but a broad treatment to aquaint the reader with the general state of the art. Many of the references cited contain extensive bibliographies with which the subject may be pursued in more detail.

# 3. RESEARCH EFFORTS

## 3.1 Discussion of Analytical Concepts

In studying the change in fluid behavior or basic mechanisms between 1-g and 0-g, one is led to examine the change in forces or force levels in going from one gravity field to the other. In general, the forces acting on a liquid are the inertial forces and the intermolecular forces, which are exhibited in the form of the surface-tension forces. Under 1-g or earthbound conditions a liquid in a container is restrained from accelerating freely in the gravity field. Under these conditions the inertial forces predominate, and only small effects of the surface-tension forces are noticeable. Typically, the effects of dominant inertial forces are the shaping of liquids in tanks, the weight of the liquid, the hydrostatic pressure of liquid columns, the rise of vapor bubbles in liquids due to buoyancy, and the convection currents in liquids as a result of heat inputs. Although the surface-tension forces are small in comparison with inertia forces at 1-g, their effects are still observable in the meniscus of liquids in contact with solid bodies and in the capillary rise or depression in small diameter tubes.

When a liquid or a system containing liquid and vapor is allowed to accelerate freely in the local gravity field, the inertia forces disappear and the surface-tension forces remain. These forces are dominant in determining the equilibrium configuration and the liquid configuration dynamics, and they play a larger role in the heat-transfer mechanics. Research concerning the behavior of fluids in a weightless environment has therefore involved study of surface-tension or surface-energy phenomena and of

their effect on fluid behavior.

### 3.1.1 Early History of Surface-Energy Studies

The history of the study of surface-tension phenomena can be traced as far back as Leonardo da Vinci and Sir Isaac Newton. It was Young, however, who first established the theory by demonstrating how the principles of surface tension and contact angle can be used to explain a great many capillary phenomena. The theory was put on a firm mathematical foundation by Laplace and later Poisson. Further developments were made by Gauss, who applied the principle of conservation of energy to the system and obtained not only the equation of the free surface but also the conditions of the contact angle. Other earlier investigators include Dupre, Rayleigh, Gibbs, and Plateau, who utilized soap bubbles and other devices to determine the equilibrium configuration of liquids. Later investigations were carried out by Langmuir and Harkins in the United States and by Adam and Burdon in England

### 3.1.2 Liquid Contact Angle

Consider a liquid in contact with a solid surface as shown in Fig. 2. The free surface energies at the solid liquid-vapor interfaces may be represented by the surface-tension forces acting in the direction of the surfaces. The angle at which the liquid meets the solid surface, measured in the liquid, is the contact angle.

For the liquid to be in equilibrium with the solid surface, the surface-tension forces at the solid liquid-vapor interfaces must be in balance parallel to the solid surface. Therefore,

$$\sigma_{vs} = \sigma_{ls} + \sigma_{vl} \cos \theta \tag{1}$$

and

$$\theta = \cos^{-1} \frac{\sigma_{vs} - \sigma_{ls}}{\sigma_{vl}} \tag{2}$$

where $\sigma_{vs}$, $\sigma_{ls}$, and $\sigma_{vl}$ are the surface tensions, or surface energies, of the vapor-solid, liquid-solid, and vapor-liquid interfaces, respectively, and $\theta$ is the contact angle. (Equation (1) is known as the Young-Dupre equation.) It is observed that the contact angle depends on the magnitudes of the three surface-tension forces. When $(\sigma_{vs} - \sigma_{ls})/\sigma_{vl}$ is between 0 and 1, the contact angle lies between $0^{\circ}$ and $90^{\circ}$, and the common convention is to call the liquid a wetting liquid. If, however, $(\sigma_{vs} - \sigma_{ls})/\sigma_{vl}$ lies between 0 and -1, the contact angle will lie between $90^{\circ}$ and $180^{\circ}$, and the liquid is said to be nonwetting liquid. The contact angle should remain constant in any gravity field, including a weightless environment, because the intermolecular forces that are exhibited in the surface-tension forces are independent of the level of the gravity field.

### 3.1.3 Pressure Difference Across the Liquid-Vapor Interface

Although the property commonly referred to as surface tension is an energy, it behaves in every way like a tension and tries to make the surface as small as possible. Thus a drop of liquid tends to become spherical, and the tendency of the surface to contract increases the pressure inside the drop. Because the pressure everywhere inside the drop is the same, this pressure difference between the inside and outside of the drop is the

pressure drop across the interface and is given by the following expression:

$$\Delta P = \frac{2\sigma}{R} \tag{3}$$

where R is the radius of the drop or more generally the radius of curvature of the interface for a spherical interface. This expression is found everywhere in the literature and is simply derived by equating the surface-tension force acting along a meridian circumference to a pressure difference times the circular area enclosed by this meridian circumference. If the interface is not spherical, the pressure drop is given by the more general equation

$$\Delta P = \sigma \left( \frac{1}{R_1} + \frac{1}{R_2} \right) \tag{4}$$

### 3.1.4 Dimensionless Parameters

Dimensionless parameters have been employed in the field of fluid mechanics to describe behavior similarities between systems of different size and to define different behavior regions. For instance, Reynolds number and Rayleigh number define the conditions required to obtain similar flow and convection current characteristics, respectively, in different sized systems, and they also define regimes of different behavior. Other dimensionless parameters that have been found useful in the field of fluid mechanics are Grashof number, Prandtl number, Froude number, Nusselt number, Mach number, etc. These parameters are useful to the theorist in providing an insight into the basic behavior mechanism and useful to the engineer when studying the behavior of full-sized systems through the use of models.

Two dimensionless parameters that are useful in the field of capillarity are Bond number, the ratio of gravitational or acceleration forces to capillary or surface-tension forces, and Weber number, the ratio of pressure or inertia forces to surface-tension forces. These parameters are defined in terms of the physical constants of the system as follows:

$$Bo = \frac{F_a}{F_c} = \frac{Ma}{\sigma L} = \frac{\rho L^3 a}{\sigma L} = \frac{\rho}{\sigma} L^2 a \tag{5}$$

$$We = \frac{F_i}{F_c} = \frac{(\text{Pressure drop})(\text{Area})}{\sigma L} = \frac{1/2\ \rho V^2 L^2}{\sigma L} = \frac{\rho}{\sigma} V^2 L \tag{6}$$

where $\rho$ is the liquid density, $L$ is a dimension characteristic of the system, $a$ is the acceleration imposed on the system (equals 1-g when at rest on Earth), and $V$ is the local flow velocity.

Bond number (Eq. (5)) defines the acceleration or gravity regimes in which either acceleration or capillary forces dominate. For instance, when the Bond number is larger (greater than one) acceleration forces dominate, whereas when the Bond number is small (less than one) the surface-tension forces will be dominant in determining the fluid mechanisms. Bond number should also be useful in predicting the critical acceleration of the liquid gas interface.

Weber number (Eq. (6)) defines the behavior of the interface in the presence of flow forces. When the Weber number is large the flow forces predominate and the capillary forces are insignificant, whereas when the Weber number is small the capillary forces will shape the interface. By rearranging the expression for Weber number an indication of the transition time for zero-gravity phenomena, such as interface formation or wave

period, may be obtained:

$$We = \frac{\rho}{\sigma} V^2 L = \frac{\rho}{\sigma} \left(\frac{L}{T}\right)^2 L = \frac{\rho}{\sigma} \frac{L^3}{T^2} \tag{7}$$

$$T = \left(\frac{\rho}{We\sigma}\right)^{1/2} L^{3/2} \tag{8}$$

The value of Weber number will be empirical depending on the specific configuration.

Reynolds [1] has portrayed the various hydrodynamic regimes as a function of Bond and Weber numbers as shown in Fig. 3, which is taken from his work. A new dimensionless parameter is introduced in this diagram--namely, the Froude number, which is the square root of the ratio of Weber number to Bond number. It defines the boundary between the inertia dominated regime and the acceleration dominated regime. This diagram provides a useful means of visualizing the several hydrodynamic regimes as defined by the several dimensionless parameters.

### 3.1.5 Effect on Facility Requirements

Several types of zero-gravity facilities have been proposed such as drop towers, airplanes, ballistic rockets, orbiting vehicles, and drops from balloons, helicopters, and canyon bridges. Each of these involves the technique of free fall, or equilibrium with the local gravity field, to obtain a zero-gravity environment. Of these, the drop tower employing a drag shield around a freely-floating experiment, the airplane flown on a ballistic trajectory, and the ballistic rocket have been the most used.

The study of the various aspects of fluid mechanics in zero gravity requires zero-gravity facilities with different characteristics. For

instance, the bubble behavior produced by heat transfer is a high speed phenomenon, and only a short-time facility such as a drop tower is required. On the other hand, if the heat-transfer characteristics in a system are being studied, as in a closed propellant tank, a facility offering several minutes of zero-gravity time is required, such as a ballistic rocket. The study of forced convection mechanics, or the behavior of evaporators or condensers, requires relatively short times such as are available in drop facilities or airplanes. In these studies, the interface is generally so small that small perturbations of the order of a few milli-g's are not important as indicated by the Bond number criterion. In studying the behavior of large liquid vapor interfaces as in models of propellant tanks, however, the acceleration level provided by the facility becomes important as does the initial disturbance. If the zero-gravity time is long enough for the initial disturbance to damp out or be negated by a collection and release maneuver, however, it becomes less of a consideration.

The expressions for Bond and Weber numbers (Eqs. (5) and (6)) can be used to provide an estimate of the zero-gravity time and maximum gravity level allowable in a facility to perform interface studies. A plot of the predicted interface formation time and allowable acceleration or g level as a function of model size is shown in Fig. 4. The allowable acceleration level results from the expression for Bond number using an experimentally determined Bond number near one with L corresponding to the radius. The interface formation time is obtained from the expression for time developed from the Weber number relation using a Weber number of

one and an experimentally determined characteristic length (L). The most significant aspect of Fig. 4 is the low acceleration or g level required for interface experiments in the 2- to 20-inch range (the most desirable model range). This requirement also implies that the initial disturbance shall be low. It is this acceleration and disturbance requirement that has prevented the successful use of airplane facilities for interface experiments even though their 15-second time has been very attractive.

## 3.2 Interface Configuration

### 3.2.1 Shape and Location of the Interface

The configuration of the liquid-vapor interface under weightless conditions has been studied analytically by several investigators. Benedikt [2] and Reynolds [1]* have calculated exact solutions for the configuration of the interface between parallel plates as a function of the gravity level or Bond number and, from these calculations and the principles involved, have inferred the configuration of the interface in other geometries. Li [3] has used the principle of the minimization of the free surface energies to predict the interface configuration in many geometries. All these analyses indicate that the interface configuration is primarily dependent on the contact angle and that during weightlessness the liquid vapor interface tends to assume a constant curvature surface that intersects the tank wall at the contact angle.

The results of the calculations for the configuration of the interface between two parallel plates as obtained by Reynolds are presented in Fig. 5. The calculations present the interface configurations for a relatively wetting liquid (contact angle, $10^{o}$) and a relatively nonwetting liquid (contact angle, $140^{o}$) each at a series of Bond numbers from zero (true weightlessness) to infinity (essentially representative of 1 g). At a Bond number of zero the interface is a surface of constant curvature intersecting the wall at the contact angle. The contact angle determines whether the surface is concave or convex. The increased

*Reynolds indicated that he also found the calculations in the works of Rayleigh.

distortion of the surface from its constant curvature configuration as Bond number increases is apparent.

The results of the calculations for the two-dimensional case may be used to infer the configuration in three-dimensional geometries. Figure 6 shows the predicted configuration for cylinders and for spheres as a function of the contact angle and for the volume fraction of liquid in spheres. These predicted configurations are for a Bond number of zero. Five general configurations are shown for spheres ranging from an imbedded vapor bubble for all fillings at zero-degree contact angle to an imbedded liquid mass for all fillings at the hypothetical contact angle of $180^{\circ}$. The curved line indicates the combination of contact angles and fillings at which the interface is flat as depicted by the center diagram. The diagrams on either side of center are generally representative of the configurations obtained for the combination of contact angles and fillings in the surrounding area. The configurations predicted for cylinders do not show the end effects that would be encountered in tanks with normal ends. For tanks with hemispherical ends, the configurations may be inferred from the configuration for spheres.

Experimental verification of the predicted interface configurations has depended heavily on a suitable zero-gravity facility. The author and his colleagues conducted a series of experiments [4 and 5] in the NASA Lewis Research Center 2.3-second drop-tower facility that verified the predicted configurations. These experiments were conducted using liquids with three different contact angles in spheres, cylinders, and cones at several different fillings. The results for the range of conditions can be represented by Fig. 6; however, photographs of several

interface configurations are shown in Fig. 7. Clodfelter [6] has recently used the 1.85-second drop facility at Wright Field to confirm some of these results and has extended the work to show some interesting end effects in flat-bottomed cylinders.

### 3.2.2 Separation of Liquid and Vapor

Although the analytical and experimental results indicate that the interface configuration can be predicted for simple containers given the contact angle and ullage volume, the location of the liquid and vapor is often undesirable from the standpoint of reliable pumping and venting. This is especially true for a wetting liquid (typical of most propellants currently being considered) in spherical or nearly spherical tanks, because the location of the vapor bubble is random. Under these conditions reliable pumping and venting cannot be assured, and a substantial portion of the zero-gravity research effort is concentrated on methods of obtaining reliable separation of the liquid and vapor.

#### 3.2.2.1 Acceleration Fields

The method that is in use at the present time is the creation of an acceleration field by the use of ullage rockets. Although this method appears to work well, it becomes heavy if more than a few engine starts or venting cycles are required. Spinning the propellant tank has been proposed as a means of separating liquid and vapor but has not received much serious consideration. The use of an acceleration field to separate liquid and vapor, however, appears practical in the case of liquid separators, in evaporator tubes, and possibly in condenser tubes. In the case of liquid separators, energy from the gas and liquid stream would be used to create a centrifuge action to separate the liquid. In the

evaporator and the condenser tubes, a spiral tape inserted in the tube has been proposed. Evans [7] studied such a geometry by using bubbles in water and found the separation good.

3.2.2.2 Capillary Baffles

The analyses for defining the configuration of the interface indicated a reduction of system energy as the interface changed from its normal gravity configuration to the zero-gravity configuration. It therefore appeared promising to study the ability of tank geometries providing appreciable changes in surface energy to position the liquid and vapor in acceptable configurations. A simple configuration that probably has occurred to most investigators in the field and has been suggested and analyzed by Reynolds [1] is a tube mounted over the pump inlet concentric with the vertical centerline with holes around the bottom to allow fluid transfer between the tank and the tube as shown in Fig. 8(a). An analysis using either surface energy or capillary pressure drop can be made, which shows that a wetting liquid should rise in the tube when the tube diameter is less than one-half of the tank diameter and fall if it is greater than one-half of the tank diameter. This behavior is a positive demonstration of the tendency of the surface energy to minimize [8]. Because of this minimization of the surface energy, the liquid then takes the configuration in weightlessness shown in Fig. 8(b). The liquid is maintained over the area of the pump inlet, while the vapor is maintained in the area of the vent.

The author and his colleagues have studied the performance of this geometry in a series of experiments in the drop tower [8 and 9] and in the MA-7 spacecraft [10]. A desirable characteristic of this geometry

in spheres and to some extent in cylinders is its ability to recapture the liquid following an excessive acceleration disturbance. This effect, which is shown in Fig. 9, shows the results of drop-tower tests in which the standpipe baffle was at various initial angles to the gravity vector. For the 90° test the time available was insufficient to allow complete filling of the baffle. The tendency of the baffle to fill with liquid was also noted at 180°, but again the time was insufficient to allow complete filling of the baffle. The most serious shortcoming of this baffle configuration is its inability to provide reliable positioning of the vapor bubble over the vent if the standpipe is more than 50 percent of the height of the sphere. If the tank is filled to more than 83 percent the resulting ullage bubble will float free [9].

In an effort to overcome the shortcomings of the standpipe design, the geometry shown in Fig. 10 was proposed [9]. This design utilizes a sphere within the spherical tank somewhat offset in the direction of the pump inlet. The action is such that the vapor bubble tends to return to the location (over the vent) where it can become most nearly spherical (which represents the condition of minimum energy) after an excessive acceleration. For a geometry in which the inner sphere is 50 percent of the tank diameter and the offset is 10 percent of the tank diameter, the tank can be filled to 95 percent without the ullage bubble floating feee. The tapering sections provide a stable interface position around the tank as it empties, and the geometry provides an excellent resistance to vapor pull-through during pumping in addition to the capability of complete volume pump-out. By mounting the inner sphere on webs between it and the lower half of the tank, an even stronger pumping geometry is created.

### 3.2.2.3 Screens

The use of screens has been proposed as a means of trapping a sufficient quantity of propellant over the pump inlet to start the engine. The staff of the Bell Aerosystems Company [11] has made an extensive study of the ability of screens to retain propellants over the pump inlet. In all cases, small mesh screens were employed that were capable of retaining liquids in model tanks in a normal-gravity field. A screen configuration that was studied intensively is shown in Fig. 11 (taken from [11]). When the acceleration is directed normal to the screen as in Fig. 11(a), the screen lies in an equipotential surface of the acceleration field, and the volume trapped behind the screen is equivalent to a closed tube with a screen across the open end. The small mesh screens stabilize the surface while the actual holding force is provided by the ullage gas pressure as shown in the enlarged section. In this configuration a screen with a mesh of approximately 0.1 inch should be capable of retaining liquid against an acceleration equivalent to normal gravity. The ability of screens to retain propellant against transverse vehicle accelerations as shown in Fig. 11(b) is much less than for normal accelerations. This configuration is more analogous to an open tube with a stabilizing screen across one end. In this case, there is a head difference subject to the acceleration that, in turn, sets up a pressure difference that then must be retained by the pressure difference developed across the interface in the screen openings as shown in the enlarged section. The mesh of screens to resist transverse accelerations must be much finer than for normal accelerations because of this differential head.

Two configurations using screens that appear promising are shown in Fig. 12 (taken from the Bell study [11]). Of these the spiral hose design appears more promising because of its ability to achieve complete bubble-free expulsion for any filling of the tank. It is interesting to note that in this configuration the ability to retain propellant against adverse vehicle accelerations is equal for the transverse and axial directions.

Screens do not provide positioning of the vapor bubble over the vent except for very complicated geometries involving multiple screens, which appear to have shortcomings in obtaining complete expulsion. Their main advantage appears to be the ability to resist a higher acceleration disturbance than baffle systems for a given weight.

#### 3.2.2.4 Dielectrophoresis

The principle of dielectrophoresis has been proposed as a means of orienting or positioning the liquid and vapor in the propellant tank. When a dielectric liquid and vapor are placed in a nonuniform electric field the liquid will tend to move into the region of highest field strength. This principle has been well known for some time and can be found in texts on classical electromagnetics. Blackmon [12] has studied the application of the principle to the positioning of liquid in a propellant tank both analytically and experimentally and has demonstrated collection into predicted configurations. The staff of the Bell Aerosystems Company [11] has also made a study of systems employing dielectrophoresis to position liquid in the tank. Their experiments included the measurement of the pressure induced by the electric field, which they found to be variable and not completely predictable. Thus,

while they agreed that liquid could be collected in an electrode system in zero gravity, they could not predict the ability of the system to retain the liquid against a random acceleration. It appeared that the induced pressure inconsistencies may have been due to practical geometry problems causing unwanted field concentrations and to time and temperature variation of the electrical properties of liquids. The conclusions from both investigations were that dielectrophoresis may be a useful effect, but that more knowledge concerning the electrical properties of the liquids and more development is necessary.

3.2.2.5 Temperature Gradient

A physical effect that may be useful in the separation of liquid and vapor during weightlessness makes use of the dependence of surface tension on temperature. The surface tension decreases with temperature until it reaches zero at the critical temperature where the fluid phases and, therefore, the interface are not separately definable. If a vapor bubble is located in a liquid in which there is a temperature gradient, the temperature of the liquid vapor interface will be higher at one pole of the bubble than at the other. Under this situation the liquid in the warmer interface where the surface tension is lower will flow to the region of colder temperature and higher surface tension. This effect constitutes a movement of the vapor bubble from cold to warm regions.

The phenomenon has been studied in experiments by Young, Goldstein, and Block [13] in which bubbles were restrained from rising in a normal-gravity field by a sufficiently high temperature gradient. Their results indicate that although the effect is not normally noticeable at normal gravity because of strong buoyancy effects, it may be useful in or near

zero-gravity conditions. Because the bubbles tend to stay at a warm surface, it may be an unwanted effect in heat-transfer systems.

### 3.3 Interface Dynamics

The previous discussion has been concerned mainly with the configuration of the interface, the location of the liquid and vapor, and the means of influencing the configuration or location under the condition of no external disturbances to the system. When disturbances such as attitude control accelerations or outflow disturbances are imposed, however, the established interface or fluid configuration will be distorted or disturbed. If the disturbance is sufficiently large, the established interface may break, and the liquid, therefore, will move to a new position. The dynamic behavior of the interface in response to these disturbances is of importance because of its affect on various propellant management problems, such as pumping and venting operations, and on the stability of the attitude control system. It is expected that Bond and Weber numbers will be of significance in describing dynamic behavior because they incorporate the effects of acceleration, inertia, and surface energy.

#### 3.3.1 Interface Formation Time Following a Change in Acceleration Level

One phase of interface dynamic behavior that has been under study is the time required for the interface to form its zero-gravity configuration after release from a normal-gravity or high-acceleration field. Benedikt [14] derived an expression for the oscillation time of an initially deformed freely falling mass of liquid. Functionally his expression is equivalent to the expression for Weber number, and it indicates that the transition time is a function of the ratio of density to surface tension

to the one-half power and of a characteristic dimension of the interface to the three-halves power. It is similar to an expression for the oscillation frequency of a liquid jet issuing from a noncircular hole derived by Rayleigh [15].

The author and his colleagues have conducted drop-tower experiments in which the time required for the interface to form in spheres and cylinders after entering zero gravity was measured, which confirmed the functional relationship suggested by Benedikt. The results of these experiments are presented in Figs. 13 and 14. The formation time given in these experiments is that required for a point on the interface and on the vertical axis of the container to move from the 1-g to the 0-g position as depicted by the small diagrams.

The general expression for formation time as a function of fluid properties and dimensions of the system derived from the Weber number by substituting a length divided by time is rearranged as follows:

$$T = \left(\frac{1}{We}\right)^{1/2}\left(\frac{\rho}{\sigma}\right)^{1/2}(CD)^{3/2} \qquad (9)$$

where $D$ is the diameter of the container, $C$ is an empirical constant, and the other symbols are as defined previously. Equation (9) indicates that formation time should vary with $D^{3/2}$ and with $(\rho/\sigma)^{1/2}$. The solid lines on Figs. 13(a) and 14(a) are drawn at a three-halves-power slope. The solid lines on Figs. 13(b) and 14(b) are drawn at a one-half-power slope. In each case the data fit the lines closely, which indicates a good correlation with theory. If a Weber number of one is assumed, then the term $CD$ may be considered the characteristic dimension of the system. For spheres, the value of $C$ was determined at 0.292 and for cyl-

inders at 0.277. Although the size range is small as limited by the drop-tower time, good correlation with theory inspires confidence in the use of the Weber number expression to predict the time response in large vehicle tanks.

As part of this program studying the interface formation time, experiments were conducted [8] in which the velocity in capillary tubes was measured. Such information is useful for determining the interface formation time in tanks employing capillary tube baffles such as in Fig. 8. A part of the results of this study is presented in Fig. 15(a) where the variation of height of the liquid in the capillary tube with time in zero gravity is given for several tube diameters. The tank diameter for these experiments was 7 centimeters. The solid lines are analog computer solutions of the equation

$$\ddot{Z} = \frac{\frac{2\sigma \cos\theta}{\rho}\left(\frac{1}{R_c} - \frac{1}{R_t - R_c}\right) - \frac{1}{2} K\dot{Z}^2 - \frac{8\nu(l_t + Z)}{R_c^2}\dot{Z}}{\left(1 - \frac{A_t^2}{A_a^2}\right)Z + l_t + \frac{A_t}{A_c} l_c + \frac{A_t}{A_a} l_a} \qquad (10)$$

for liquid rise as a function of time. A schematic drawing showing the system geometry from which Eq. (10) was derived is shown in Fig. 15(b). This equation was derived from Newton's fundamental force-mass relation and accounts for forces due to surface tension, entrance losses, and friction drag. This equation involves no empirical constants and can be evaluated from the physical constants of the system with the exception of the constant $K$ applied to the entrance loss term, which is calculated by approximate means. In the solutions shown in Fig. 15(a) this

constant was taken as 2.28, as calculated by Langhaar [16] for the entrance loss to viscosimeter tubes.

The correlation of the data with the analysis was found to be satisfactory for variations in tube diameter and initial height of liquid in the tube. The degree of correlation indicates that Eq. (10) incorporates the principal physical phenomena and is useful for calculating the velocities and displacements in capillary systems in zero gravity.

3.3.2 Interface Behavior During Outflow Disturbance

A large portion of the zero-gravity research work has been given to the determination of means of assuring that liquid is located over the pump inlet prior to engine starting. Comparatively little work has been devoted, however, to a study of the effect of the outflow disturbance on the interface nearest to the outlet. There is an almost complete absence of literature reporting either analytical or experimental studies of the phenomena. A recent paper by Povitskii and Lyubin [17] has analyzed the velocity along the free surface of the interface as affected by outflow velocity. The results of their analysis indicates that for liquid depths greater than the diameter of the outlet tube, the free surface is not appreciably disturbed beyond a diameter corresponding to four times the depth.

Because the outflow velocity creates a velocity gradient in the liquid above the outlet that appears to carry through to the interface, it is expected that the Weber number may be the scaling relation useful in relating the distortion of the interface between various system sizes. For more severe velocity gradients and greater distortions, however, the

viscosity may have an effect so that the Reynolds number may also be required to properly scale the phenomena.

The author and his colleagues have conducted outflow experiments under zero-gravity conditions in the drop tower to study the behavior of the interface under this disturbance and to attempt to determine a scaling parameter. At the present time experiments have been conducted only with flat-bottomed cylinders and one ratio of outlet diameter to tank diameter in three sizes. The results of these studies are shown in Fig. 16 where the velocity at which the interface distorts from center to circumference is shown as a function of the velocity in the outlet tube and the tank diameter.

The small diagrams depict the types of interface distortion observed. The diagram with the hemispherical interface, strictly speaking, represents only the zero differential velocity line where all points on the interface move downward at the ratio of outlet tube area to tank area (1/100) times the outlet velocity. The severely distorted interface represents the situation in which the central core of liquid is pulled through the liquid, which corresponds to high differential interface velocities and is considered unsatisfactory. The center diagram is the compromise representing some distortion but generally satisfactory for pumping.

The intersections of the lines through the data with the zero differential velocity axis were obtained by computing the undistorted interface velocity at each tank diameter for a Weber number of one and plotting the point at the outlet velocity that created it (100:1). Lines using such a zero point appear to fit the data well. A line for a Weber

number of 15, computed using the differential interface velocity, was found to represent the demarcation between slight distortion and severe distortion. Its position is shown in Fig. 16. A Reynolds number line of 2000, again calculated using differential interface velocity, is also shown, but it did not delineate the distortion regions.

If the outlet velocity corresponding to the intersection of the line for a Weber number of 15 with the data for a given diameter is considered a maximum allowable outlet velocity for that diameter, these intersections may be useful for predicting maximum outlet velocities for larger tank diameters. A plot of maximum outlet velocity as a function of tank diameter is shown in Fig. 17. The portion of the line for the larger tank diameters is drawn at a slope of one-half, which would represent a Weber number scaling parameter. Although the data tend toward a slope of one-half as shown, data for larger tank diameters are needed to verify this contention. Unfortunately, such data are impossible to obtain in present drop facilities.

### 3.3.3 Interface Behavior During Acceleration Disturbance

There are a number of acceleration disturbances that will occur in connection with the operation of space vehicles such as those resulting from attitude control system operation, crew movements, docking jolts, and atmospheric drag. The acceleration perturbation may be intermittent as in the case of attitude control operation or steady as in the case of drag or of liquid collection by thrust preparatory to engine starting. These disturbances will occur at all angles to the vehicle thrust axis and will tend to move the liquid opposite to the direction of the acceleration. The surface-tension forces give the interface the ability to resist or be

stable to a certain amount of acceleration, which is expected to be defined by the Bond number criterion (the ratio of acceleration to surface-tension forces). The study of interface behavior in response to acceleration disturbances may be divided for convenience into two phases, one for acceleration disturbances less than, and one for disturbances greater than a critical value at which the stability limit of the interface is exceeded.

There is a great deal of literature starting with Maxwell in 1890 and continuing with the contributions to hydrodynamics by Lamb and the contributions to surface stability by Taylor that can be applied to the definition of the behavior in response to accelerations less than the critical value. The great majority of it deals with the situation in which the acceleration is directed perpendicular to the interface from the less-dense to the more-dense fluid. The classical approach to the problem of hydrostatic stability has consisted in examining the character of the solution of the equations of disturbances applied to the interface. If the exponents of the series solution are pure imaginary, the disturbed interface will oscillate in time, and the undisturbed state of the interface is considered stable. If the exponents are real, the disturbance is unbounded in time, and the undisturbed state is considered unstable. The required boundary condition is a fixed contact angle at the wall. In the case of disturbed equilibrium, this leads algebraically to the usual criterion of minimum potential energy as a necessary condition for stability. Variational techniques have been used in minimizing the sum of the gravitational and free-surface potentials subject to the constraint of constant liquid volume. The resultant Euler differential equation is solved con-

sistent with the required boundary conditions. The solutions are necessarily approximate, largely because of the nonlinearity of the differential equations and the difficulty encountered with a rigorous mathematical formulation for a $0^{\circ}$ contact-angle boundary condition.

These analyses have been primarily interested in studying the dynamics of the interface and have, in the course of these studies, determined the stability limit of the interface--that is, the value of the acceleration at which the interface will break. As noted, this point is expected to be defined by Bond number, and the value obtained is called the critical Bond number. The various analyses in the literature quote values of critical Bond numbers from 0.15 to the value of 14.68 obtained by Maxwell. Recently, Masica [18] measured the critical Bond number in cylindrical tubes using the normal gravitational field as the acceleration disturbance. Part of his results are shown in Figs. 18 to 20 for different orientations of the acceleration field and position of the interface relative to the edge of the tube. The critical diameter is shown as a function of the specific surface tension $\sigma/\rho$. The left axis intercept of the solid line approximating the data is proportional to the critical Bond number and is computed as follows using Fig. 18 as an example. The equation of the solid line that is drawn at a slope of one-half is, after converting the critical diameter to centimeters,

$$D = 0.184 \left[\frac{\sigma}{\rho a(0.01)}\right]^{1/2} \tag{11}$$

When arranged in the form of the Bond number expression (Eq. (5)) and substituting the radius for the diameter, Eq. (11) becomes

$$\left[\frac{0.184}{(2)(0.1)}\right]^2 = \frac{\rho}{\sigma} aR^2 = 0.84 = Bo_{critical} \qquad (12)$$

The Bond number (based on a radius) of 0.84 agrees with the value obtained analytically by Bretherton [19] and that obtained experimentally by Hattori [20] for this configuration and acceleration direction. A variation in Bond number depending on the specific surface tension was observed for the situation in which the acceleration was directed normal to the axis of the cylinder as shown in Fig. 19. The value was 1.12 for specific surface tensions less than 43 $cm^3/sec^2$ and 2.53 for specific surface tensions greater than 43 $cm^3/sec^2$. For the configuration in which the liquid was at the edge of the tube as shown in Fig. 20, a strong edge effect was noted in that the Bond number was 3.37.

In these experiments the specific surface tension was varied over a 6:1 range, thus establishing its functional relationship in the Bond number expression. The experiments were performed, however, with only one acceleration disturbance--that of the normal gravitational field. These experiments have recently been extended in drop-tower experiments to include acceleration fields equivalent to one-tenth and one one-hundredth that of normal gravity for the configuration of Fig. 18. Acceleration forces on the container and gravitational body forces on the liquid were treated as equivalent. The results of these experiments are presented in Fig. 21. These data fit an extension at the same slope of the solid line in Fig. 18 and establish the functional relationship of acceleration in the Bond number expression.

The results of these experiments can be used to predict the critical acceleration for the interface in large vehicle propellant tanks. Fig-

ure 22 presents the critical acceleration in g's as a function of tank diameter in inches for a specific surface tension of 28.28 $cm^3/sec^2$, which is representative of many propellants. The data obtained at one, one-tenth, and one one-hundredth g are shown. The critical acceleration for vehicles of 100 to 400 inches in diameter is indicated as $10^{-6}$ to $10^{-7}$ g's.

There is very little in the literature reporting studies of the behavior of the interface in an acceleration field sufficient to break the interface. However, the work of Taylor [21] and Bretherton [19], which is a study of the motion of long bubbles in tubes, can be applied. No experimental verification is apparent in the literature as yet. It is known [22], however, that some experiments at normal gravity are being performed. Masica is also studying the phenomena at one one-hundredth g in the drop tower. The phenomena will be encountered in situations in which the drag exceeds the critical value of the interface, or during collection of liquid from possible adverse positions in the tank preparatory to engine restart, or during excessive attitude control disturbances or docking jolts. No work is apparent on the behavior as it gathers in the vapor end of the tank.

### 3.4 Heat Transfer

There has been a great deal of interest in the change in the heat-transfer mechanism in a weightless environment. The mechanism of heat input to a tank under space conditions corresponds to that of a classical pool-boiling situation, the various regions of which are shown in Fig. 23 for a 1-g field. The coordinates are heat flux plotted as a function of temperature difference.

The heat-transfer regions start with conduction at very low flux, and, as flux is increased, progress through convection and nucleation, and finally, at very high flux, progress to the mechanism of film boiling. The regions of convection and nucleation may be substantially affected by the loss of gravity. Convection currents should certainly be absent in a zero-gravity environment, although residual currents may persist for some time. The nucleation regime may be markedly affected by changes in the gravity field because of the dependence of bubble velocity on buoyancy. If the velocity becomes zero because of loss of buoyancy, the nucleation region may be replaced by a film mechanism of boiling. This situation would be predicted by the Rohsenow [23] nucleation concept, which is gravity dependent. A nucleation model has been proposed by Forster and Zuber [24] that may be independent of gravity in that bubbles are removed from the surface by a flow field set up around the bubble because of its rate of expansion. If this model is correct, the nucleation region should be relatively unaffected by a zero-gravity environment and would probably extend down to cover the convection region. Siegel [25] performed the first low-gravity experiments studying the pool boiling mechanism under several gravity fields from essentially zero to one. He was primarily interested in studying photographically the change in ebullition and vapor removal. During a discussion of his paper [26] presented to the ASME, he stated that in the nucleation regime he noted no change in the temperature difference obtained at a given heat flux, which tends to support the nucleation concept that is independent of gravity.

A series of experiments using liquid hydrogen has been performed by General Dynamics/Astronautics [27] in which the heat transfer in the

nucleate range as a function of temperature difference was measured at 1-g and 0-g conditions. Results of this study are shown in Fig. 24. These results indicate that zero gravity has little effect on heat transfer in the nucleate region, which supports the nucleation model that is independent of gravity. The experiments by Merte and Clark [28] using liquid nitrogen have also tended to support the nucleation concept that is independent of gravity.

The primary effect of the heat-transfer mechanism that is of interest in space vehicle propellant tank systems is the pressure rise within the container. This pressure rise is difficult to calculate because of the uncertainty in the liquid configuration, the variation in the direction of the radiant heat source, and the uncertainty about the heat-transfer mechanisms that may apply to the liquid and vapor portions of the tank even though the mechanism in the liquid seems reasonably well established. In comparing pressure rise data at 1-g and 0-g, it has been found convenient to compare the actual pressure rise with that which can be calculated by making several different assumptions about the heat distribution within the tank. The position that experimental data assumes in relation to the theoretical models on a pressure against heat added plot is then an indication of how the energy is being distributed within the tank. Figure 25 is a plot of pressure against heat added for three theoretical models. The first model assumes homogeneous conditions thoughout the tank and is a common calculation that is performed to compare data of this type. The second model assumes that all of the energy absorbed by the dewar goes into the evaporation of liquid with the vapor phase temperature always being equal to the saturation temperature corresponding to sphere pressure

and the liquid phase temperature remaining constant at the saturation temperature corresponding to seal-off pressure. The third model is a practical upper limit on the pressure against heat added plot much as the homogeneous model is the lower limit. The third model assumes that all the energy is delivered to the vapor phase with no energy transfer at the liquid-vapor interface so that the vapor becomes superheated.

There are two important factors that would be expected to cause a different rate of pressure rise in a storage tank when normal gravity quiescent and zero-gravity tests are compared. The first factor is the change in configuration, or position of the liquid and vapor within the storage tank. As shown in Fig. 6, for a half-filled spherical tank the normal-gravity configuration has the interface bisecting the tank, while the zero-gravity configuration has a spherical interface with the tank walls totally wetted and the vapor bubble randomly located in the interior of the tank. The second factor affecting the rate of pressure rise in a storage tank is the reduction in buoyancy and convection due to the reduction in the gravity field.

For a normal-gravity test only part of the storage tank is covered with liquid so that a large amount of the heat that is added goes directly into the vapor phase. This heating of the vapor causes it to become superheated. Some of the hot vapor will come in contact with the liquid-vapor interface causing evaporation from the surface. The energy that enters the storage tank through the liquid wetted walls goes into forming bubbles and superheating the liquid in a thin layer directly adjacent to the wall. Convection currents will carry the hot liquid to the surface where evaporation takes place, and buoyancy will cause the bubbles to

rise rapidly to the liquid-vapor interface and join the vapor space. Because the bubbles rise rapidly through the liquid there is little condensation and consequently little heating of the liquid. The surface evaporation model is based on the assumption that all of the added heat goes into evaporating liquid with no heating of the remaining liquid. Consequently, depending on the heat-transfer rate and distribution, it would be expected that experimental normal-gravity quiescent pressure rise data would be clustered around the surface evaporation model theoretical line. It would also be expected that high heat-transfer rates or heating only from the top of the tank would cause faster pressure rises than the model predicts, and that low heat-transfer rates or heating only from the bottom of the tank would cause lower pressure rises than the model predicts.

Initially during a zero-gravity test the walls of a spherical storage tank would be liquid wetted. Consequently, in contrast to the normal-gravity quiescent test, there will be no direct heating of the vapor phase, and the bubbles that form on the wall of the tank will be faced with some depth of liquid to penetrate in order to reach the vapor space. The bubbles will pinch off the wall due to dynamic forces that, for most cryogenic liquids, are much greater than buoyant forces even under normal-gravity conditions. Because of the absence of gravitational forces, it is expected that the bubbles will tend to drift rather slowly in the subcooled liquid and condense, thus giving their energy to the liquid. A nearly homogeneous condition should be the result.

There are many zero-gravity configurations that will not have totally wetted tank walls due to tank geometry, internal baffles, and the use of ullage control rockets. Also, in spheres and other normally totally

wetted configurations, the possibility exists that the vapor bubble may drift to one side of the tank. If the evaporation rate is higher than the rate at which the surface can be rewetted, a dry spot will appear and grow until the evaporation balances the inflow of liquid. Under these conditions there will again be direct heating of the vapor and higher rates of pressure rise must be expected.

The majority of the experimental work, being performed at Lewis Research Center in support of the prediction of the thermodynamic history of storage tanks containing liquid propellants, is being carried out using 9-inch-diameter dewars containing liquid hydrogen. The affect on the rate of pressure rise of several experimental variables, including the use of internal baffles, the heat flux rate and distribution, and the initial percent filling, is being explored. Rocket vehicles are being used to obtain several minutes of low-gravity environment.

### 3.5 Evaporation and Condensation

The free liquid-vapor interfaces in evaporators and condensers have not contributed to operational and performance problems as they have in the tanks of other systems. This is due to the small diameter of tubes used in evaporators and condensers (usually less than 1/2 in.), which according to the Bond number criterion makes them stable to accelerations of 0.03 g or more for the smaller tubes (0.1 g for 5/16-in. tube). Acceleration perturbations of this magnitude will not ordinarily be in the operating spectrum of the vehicle except when under boost thrust, which will permit normal operation of the system.

Because forced convection will exist in evaporators and condensers designed for minimum weight, it is unlikely that there will be any appreciable change in the heat-transfer mechanism. The possibility of generation of bubbles within the liquid in the evaporator or the inclusion of vapor in the liquid in the condenser was originally of some concern; however, the reasonably large stability of the interface and the use of counterflow heat exchangers to provide subcooling below the interface and a temperature gradient to move bubbles toward the interface has virtually eliminated these problems. Also Evans [7] has shown that either a spiral wire or a twisted tape in a tube will centrifuge liquid to the outside and increase the separation stability margin. These configurations are permissible in evaporator tubes where the pressure drop they impose has only a small effect on cycle efficiency.

Although it appears that the interface in an individual tube will have, or can be provided with, a reasonable degree of stability, there is still the problem of stability of the interface level between individual tubes in the face of acceleration perturbations from directions other than on the tube axis and directed from the liquid to the vapor. The forces available to counteract this change in level are the changes in pressure drop within the tube with change in level (condensing length) and the change in surface-tension force if the tubes are tapered and if the liquid wets the wall. However, the magnitude of the surface-tension forces are very small for practical tube sizes and tapers, which leaves the pressure drop as the main stabilizing parameter. In the evaporator where the working pressure is high, it is practical to design with a reasonable pressure drop thus providing a satisfactory ability to resist

adverse accelerations. Even so, the dimensions of the evaporator normal to the tube bundle axis should be kept as small as possible to minimize the head that must be resisted by change in pressure drop for accelerations normal to the tube axis. The situation is similar to that described for screens in propellant tanks.

The position of the condenser in the cycle does not allow as much generosity with design pressure drop as in the evaporator without serious effect on the efficiency. Thus, a substantial portion of the zero-gravity research concerned with condensers has been concentrated on the pressure-drop characteristics. The correlation that has been used for two-phase pressure drop at normal gravity is the Lockhart-Martinelli correlation [29], which involves the Reynolds number and thus the viscosity. Reynolds [1] has proposed that the effects of surface-tension be introduced into two-phase pressure-drop correlations for use at zero gravity. In his analysis, surface tension effects are introduced by assuming that the friction drag is proportional to the size of condensed droplets adhering to the wall, which increases the tube roughness. The assumption of wall bound droplets is in keeping with the tendency for the surface energy to minimize.

Most of the actual zero-gravity data obtained to date has been concerned with observation of droplet and interface behavior and only qualitative measurement of the pressure drop. No effort is apparent in the literature as yet to systematically study the pressure drop in zero gravity as a function of the various parameters and to attempt a correlation with theory. The Lewis Research Center is conducting an experimental

study (using an airplane as a zero-gravity facility) of the pressure drop in condensers with mercury as the working fluid in which several parameters are varied. This study is incomplete, but preliminary results indicate that the pressure drop in zero gravity is slightly but consistently higher than the pressure drop under normal gravity. The pressure drop in these experiments is somewhat higher than predicted by the Lockhart-Martinelli correlation at low velocities but corresponds well at high velocities.

## 4. CONCLUDING REMARKS

This paper has reviewed the analytical and experimental research directed toward the solution of the problems encountered with liquid-vapor systems in weightlessness and has presented the results of some recent experimental work studying the correlation of certain aspects of the dynamic behavior of the interface with the applicable dimensionless scaling parameters. The various problems encountered in the liquid-vapor systems were grouped into the categories of interface configuration, interface dynamics, pool boiling heat-transfer mechanisms, and evaporation and condensation phenomena.

The greatest portion of weightlessness research up to this time has been devoted to studies of the parameters defining the configuration and position of the liquid-vapor interface under the conditions of no external disturbances. The theoretical background is now extensive and has been verified by experiments. At the present time most of the work in this category is more of a development nature devoted to the application of the principles to systems to provide and maintain proper separation and orientation of liquid and vapor.

With the better understanding of the configuration and position of the interface, more attention has recently been given to the dynamic behavior of the interface. It has been found that a great deal of theoretical work dealing with fluid dynamics is applicable to zero-gravity interface behavior. A sizeable amount of experimental work verifying the theory has been performed, but a great deal (both analytical and experimental) remains to be done--especially that applicable to interface dynamics in response to

acceleration perturbations (attitude controls, docking jolts, etc.) and outflow disturbances.

A great deal of interest has been shown in the change in the heat-transfer mechanism with reduction in gravity or acceleration level. The resulting studies have approached the problem in several ways by studying the fundamental bubble mechanics, by measuring the heat flux as a function of differential temperature input, and by measuring the pressure rise in a closed system. Attempts have been made to correlate the results with existing heat-transfer theory. Although some understanding has been gained, a great deal of work remains in the area of understanding fundamental bubble mechanics.

Solutions for some of the evaporator and condenser liquid-vapor interface problems have become evident from the interface configuration and dynamics studies. The most work at the present time is concentrated on studies of the pressure drop in condensers because it is important to the efficiency of the system and to the tube-to-tube stability. Very little experimental results are available at the present time.

# APPENDIX

## SYMBOLS

| | |
|---|---|
| A | area |
| $A_a$ | annulus area |
| $A_t$ | capillary tube area |
| a | acceleration |
| Bo | Bond number |
| C,K | constants |
| D | diameter |
| F | force |
| $F_a$ | acceleration force |
| $F_c$ | capillary force |
| $F_i$ | inertia force |
| Fr | Froude number |
| L | characteristic length |
| $l_a$ | initial height of liquid in annulus |
| $l_c$ | length of connecting passage between capillary tube and annulus |
| $l_t$ | initial height of liquid in capillary tube |
| M | mass |
| P | pressure |
| q | heat flux |
| R | radius |
| $R_c$ | radius of capillary tube |
| $R_t$ | radius of tank |
| T | time |

| | |
|---|---|
| V | velocity |
| We | Weber number |
| Z | liquid rise in capillary tube |
| $\theta$ | contact angle |
| $\nu$ | viscosity |
| $\rho$ | liquid density |
| $\sigma_{ls}$ | surface energy of liquid-solid interface |
| $\sigma_{vl}$ | surface energy of vapor-liquid interface |
| $\sigma_{vs}$ | surface energy of vapor-solid interface |

REFERENCES

1. Reynolds, William C.: Hydrodynamic Considerations for the Design of Systems for Very Low Gravity Environments. Rep. LG-1, Stanford Univ., Sept. 1961.

2. Benedikt, E. T.: Epihydrostatics of Liquids in Vertical Tanks. Rep. ASG-TM-61-48, Norair Div., Northrop Corp., June 1961.

3. Li, Ta: Hydrostatics in Various Gravitational Fields. Jour. Chem. Phys., vol. 36, no. 9, May 1, 1962, pp. 2369-2375.

4. Petrash, Donald A., Zappa, Robert F., and Otto, Edward W.: Experimental Study of the Effects of Weightlessness on the Configuration of Mercury and Alcohol in Spherical Tanks. NASA TN D-1197, 1962.

5. Petrash, Donald A., Nussle, Ralph C., and Otto, Edward W.: Effect of Contact Angle and Tank Geometry on the Configuration of the Liquid-Vapor Interface During Weightlessness. NASA TN D-2075, 1963.

6. Clodfelter, Robert G.: Fluid Mechanics and Tankage Design for Low-Gravity Environment. Rep. ASD-TDR-63-506, Air Force System Command, Wright-Patterson Air Force Base, Sept. 1963.

7. Evans, David G.: Visual Study of Swirling and Nonswirling Two-Phase Two-Component Flow at 1 and 0 Gravity. NASA TM X-725, 1963.

8. Petrash, Donald A., Nelson, Thomas M., and Otto, Edward W.: Effect of Surface Energy on the Liquid-Vapor Interface Configuration During Weightlessness. NASA TN D-1582, 1963.

9. Petrash, Donald A., and Otto, Edward W.: Controlling the Liquid-Vapor Interface Under Weightlessness. AIAA Jour., vol. 2, no. 3, Mar. 1964, pp. 56-61.

10. Petrash, Donald A., Nussle, Ralph C., and Otto, Edward W.: Effect of the Acceleration Disturbance Encountered in the MA-7 Spacecraft on the Liquid-Vapor Interface in a Baffled Tank During Weightlessness. NASA TN D-1577, Jan. 1963.

11. Chipchak, D., et al.: Development of Expulsion and Orientation Systems for Advanced Liquid Rocket Propulsion Systems. Rep. RTD-TDR-63-1048, Bell Aerosystems Co., July 1963.

12. Blackmon, J. B.: Propellant Orientation in Zero Gravity with Electric Fields. Paper presented at IAS meeting, New York (N.Y.), Jan. 21-23, 1963.

13. Young, N. O., Goldstein, J. S., and Block, M. J.: The Motion of Bubbles in a Vertical Temperature Gradient. Jour. Fluid Mech., vol. 6, pt. 3, Oct. 1959, pp. 350-356.

14. Benedikt, E. T.: General Behavior of a Liquid in a Zero and Near Zero Gravity Environment. Rep ASG-TM-60-9Z6, Norair Div., Northrop Corp., May 1960.

15. Rayleigh: On the Capillary Phenomena of Jets. Proc. Roy. Soc. (London), vol. 29, no. 196, May 15, 1879, pp. 71-97.

16. Langhaar, H. L.: Steady Flow in the Transition Length of a Straight Tube. Jour. Appl. Mech., vol. 9, no. 2, June 1942, pp. A-55 - A-58.

17. Povitskii, A. S., and Lyubin, L. Ya.: Emptying and Filling Vessels in Conditions of Weightlessness. Planetary and Space Sci., vol. 11, no. 11, Nov. 1963, pp. 1343-1359.

18. Masica, William J., Petrash, Donald A., and Otto, Edward W.: Hydrostatic Stability of the Liquid-Vapor Interface in a Gravitational Field. NASA TN D-2267, 1964.

19. Bretherton, F. P.: Motion of Long Bubbles in Tubes. Jour. Fluid Mech., vol. 10, pt. 2, Mar. 1961, pp. 166-188.

20. Hattori, Sin-Iti: On the Motion of a Cylindrical Bubble in a Tube and Its Application to the Measurement of the Surface Tension of a Liquid. Rep. 115, Aero. Res. Inst., Tokyo Imperial Univ., 1935.

21. Davies, R. M., and Taylor, Geoffrey: The Mechanics of Large Bubbles Rising Through Extended Liquids and Through Liquids in Tubes. Proc. Roy. Soc. (London), ser. A, vol. 200, no. 1062, Feb. 1950, pp. 375-390.

22. Gluck, D.: Space and Information Systems Division, North American Aviation, Downey, Calif. Private Communication, Feb. 1964.

23. Rohsenow, W. M.: A Method of Correlating Heat-Transfer Data for Surface Boiling Liquids. Trans. ASME, vol. 74, no. 6, Aug. 1952, p. 969.

24. Forster, H. K., and Zuber, N.: Growth of a Vapor Bubble in a Superheated Liquid. Jour. Appl. Phys., vol. 25, no. 4, Apr. 1954, pp. 474-478.

25. Siegel, R., and Usiskin, C. M.: A Photographic Study of Boiling in the Absence of Gravity. Jour. Heat Transfer (Trans. ASME), ser. C, vol. 81, no. 3, Aug. 1959, pp. 230-236.

26. Usiskin, C. M., and Siegel, R.: An Experimental Study of Boiling in Reduced and Zero Gravity Fields. Jour. Heat Transfer (Trans. ASME), ser. C, vol. 83, no. 3, Aug. 1961, pp. 243-251; discussion, pp. 251-253.

27. Sherley, J. E., and Merino, F.: Zero-G Program. Final Rep. AY62-0031, from May 1960-Mar. 1962, General Dynamics/Astronautics, Aug. 15, 1962.

28. Merte, H. Jr., and Clark, J. A.: Pool Boiling in an Accelerating System. Jour. Heat Transfer (Trans. ASME), ser. C, vol. 83, no. 3, Aug. 1961, pp. 233-242.

29. Lockhart, R. W., and Martinelli, R. C.: Proposed Correlation of Data for Isothermal Two-Phase, Two-Component Flow in Pipes. Chem. Eng. Prog., vol. 45, no. 1, Jan. 1949, pp. 39-45; discussion, pp. 45-48.

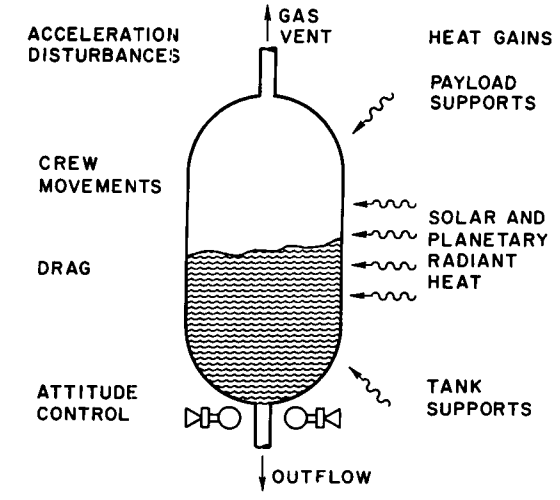


(a) Propellant tank system.

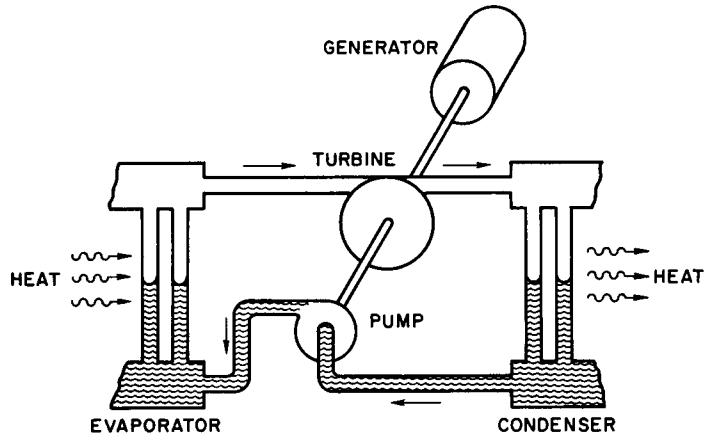


(b) Space power systems.

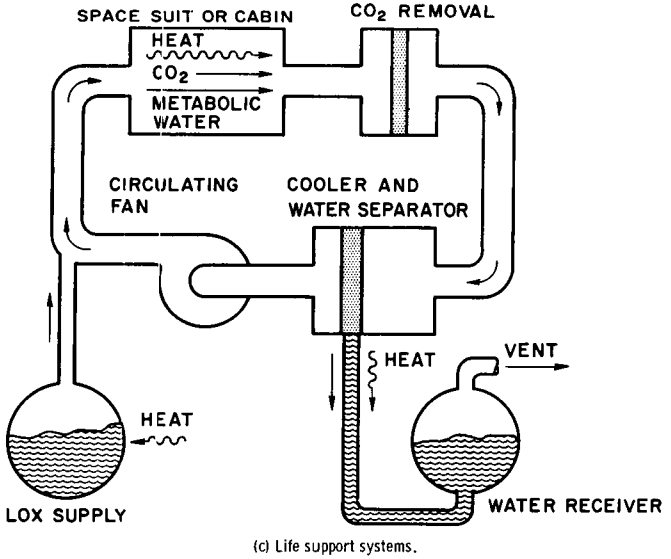


(c) Life support systems.

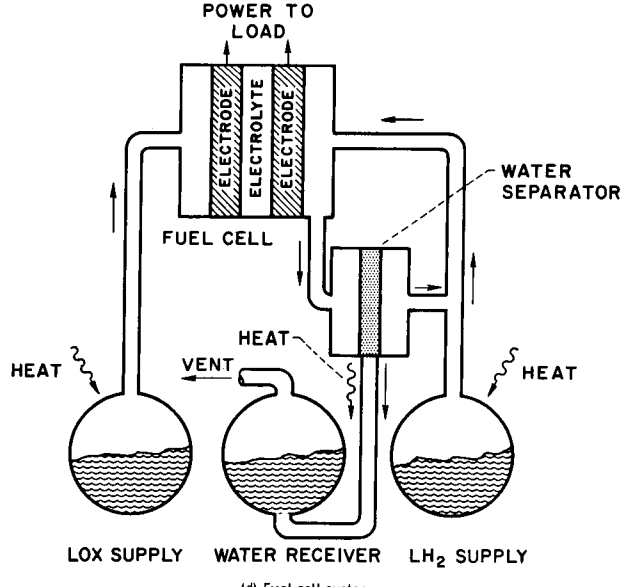


(d) Fuel cell systems.

Figure 1. - Fluid management problems in space vehicle systems.

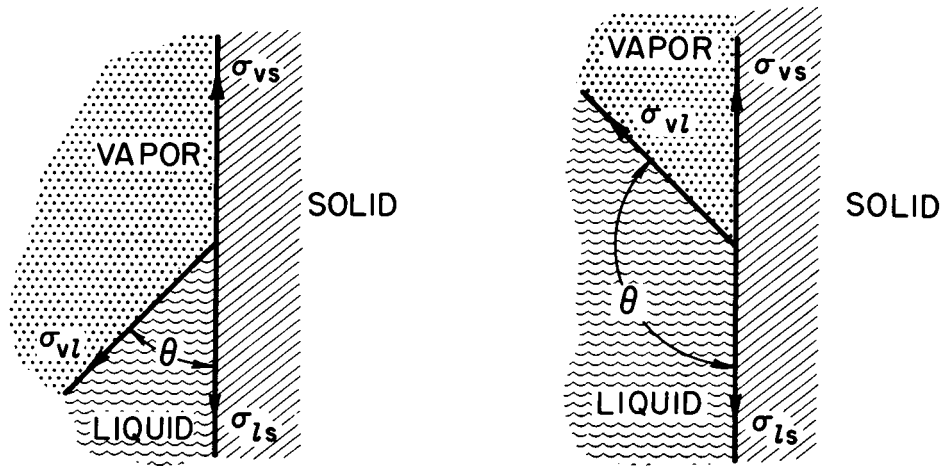


WETTING LIQUID,
$0° < \theta < 90°$

NONWETTING LIQUID,
$90° < \theta < 180°$

$$\sigma_{vs} - \sigma_{ls} = \sigma_{lv} \cos\theta$$

$$\theta = \cos^{-1} \frac{\sigma_{vs} - \sigma_{ls}}{\sigma_{lv}}$$

CS-29641

Figure 2. - Surface energy and contact angle relationship.

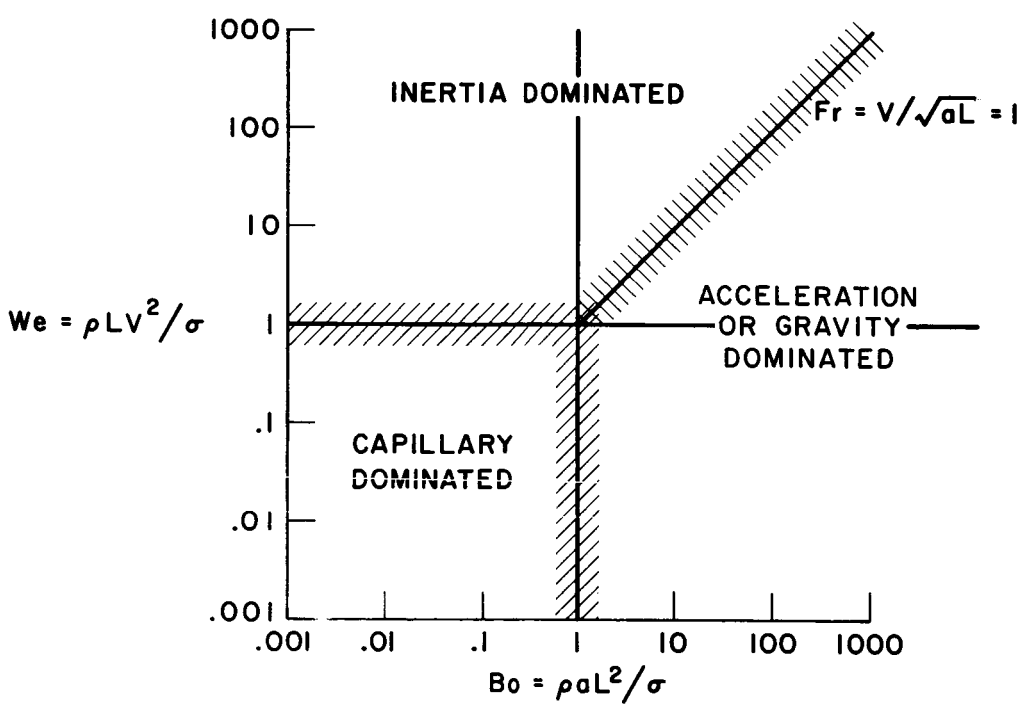


Figure 3. - Hydrodynamic regimes.

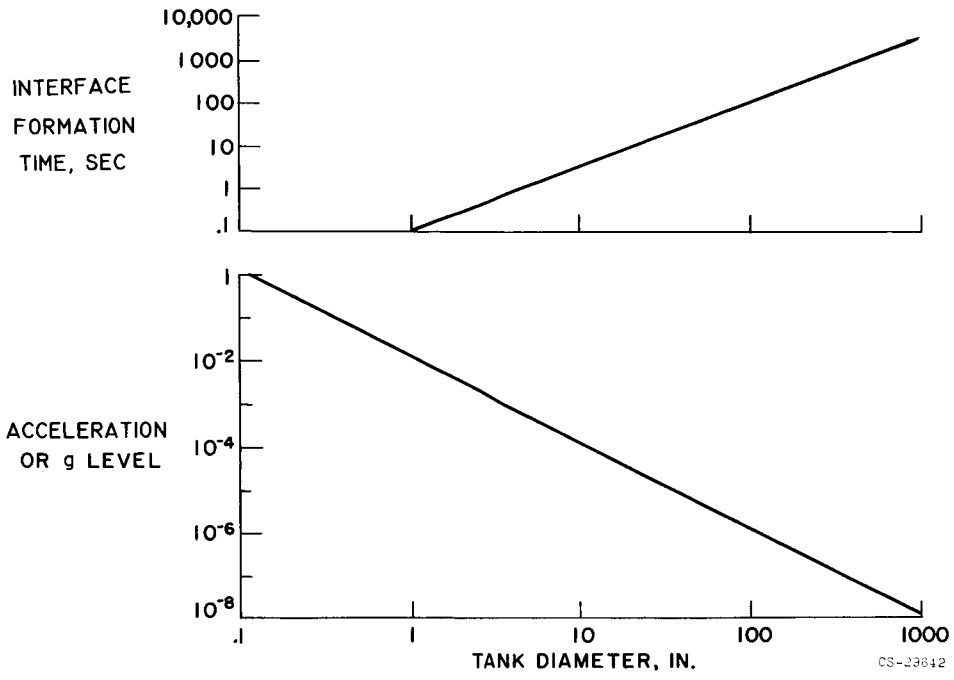


Figure 4. - Effect of model size on facility and g-level requirements.

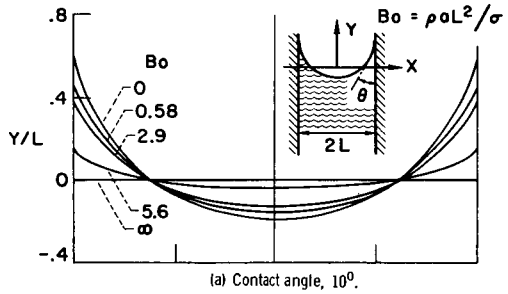


(a) Contact angle, $10^0$.

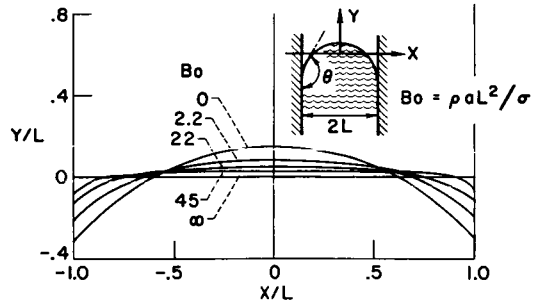


(b) Contact angle, $140^0$.

Figure 5. - Calculated configuration of liquid-vapor interface between parallel plates for various Bond numbers and contact angles.

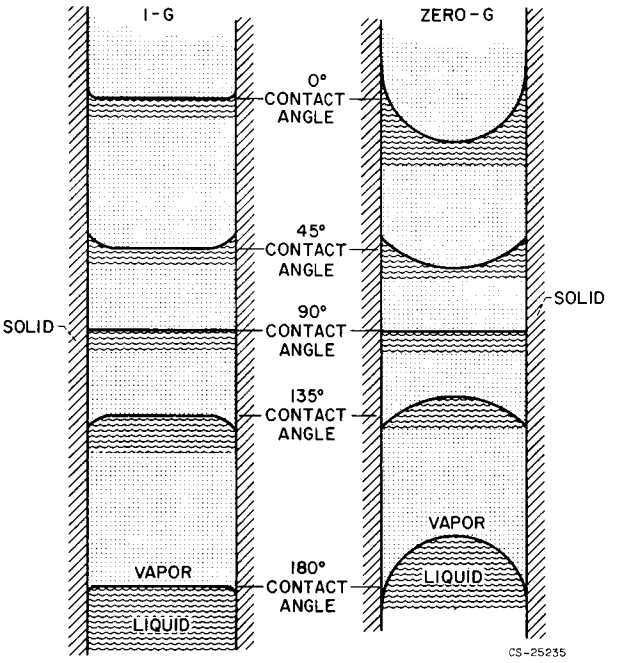


(a) Configurations in cylinders.

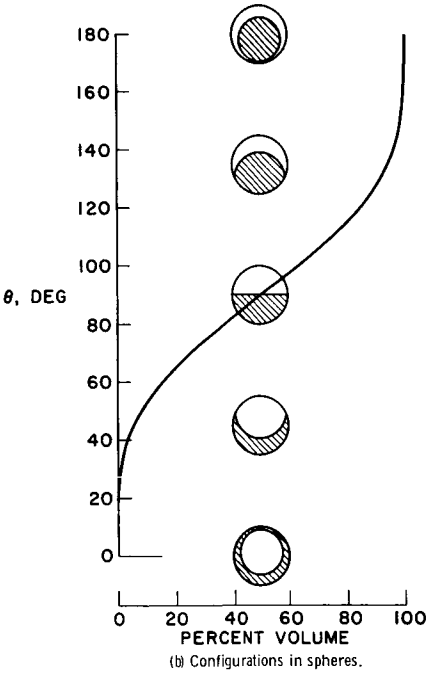


(b) Configurations in spheres.

Figure 6. - Weightlessness configuration in cylinder and spheres.

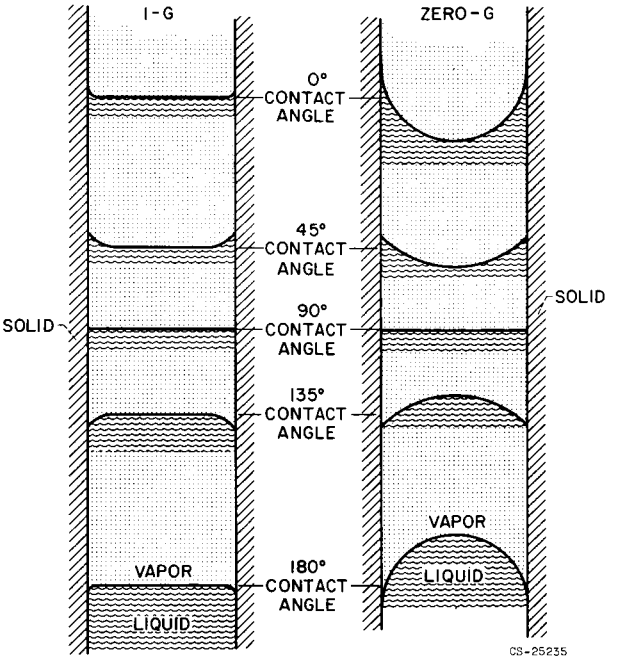


(a) Configurations in cylinders.

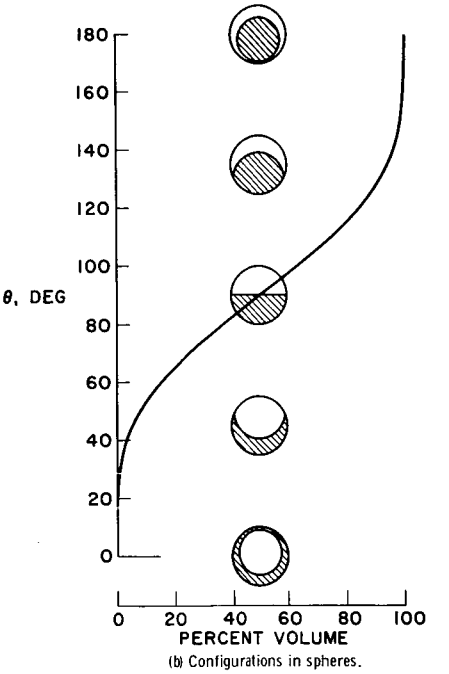


(b) Configurations in spheres.

Figure 6. - Weightlessness configuration in cylinder and spheres.

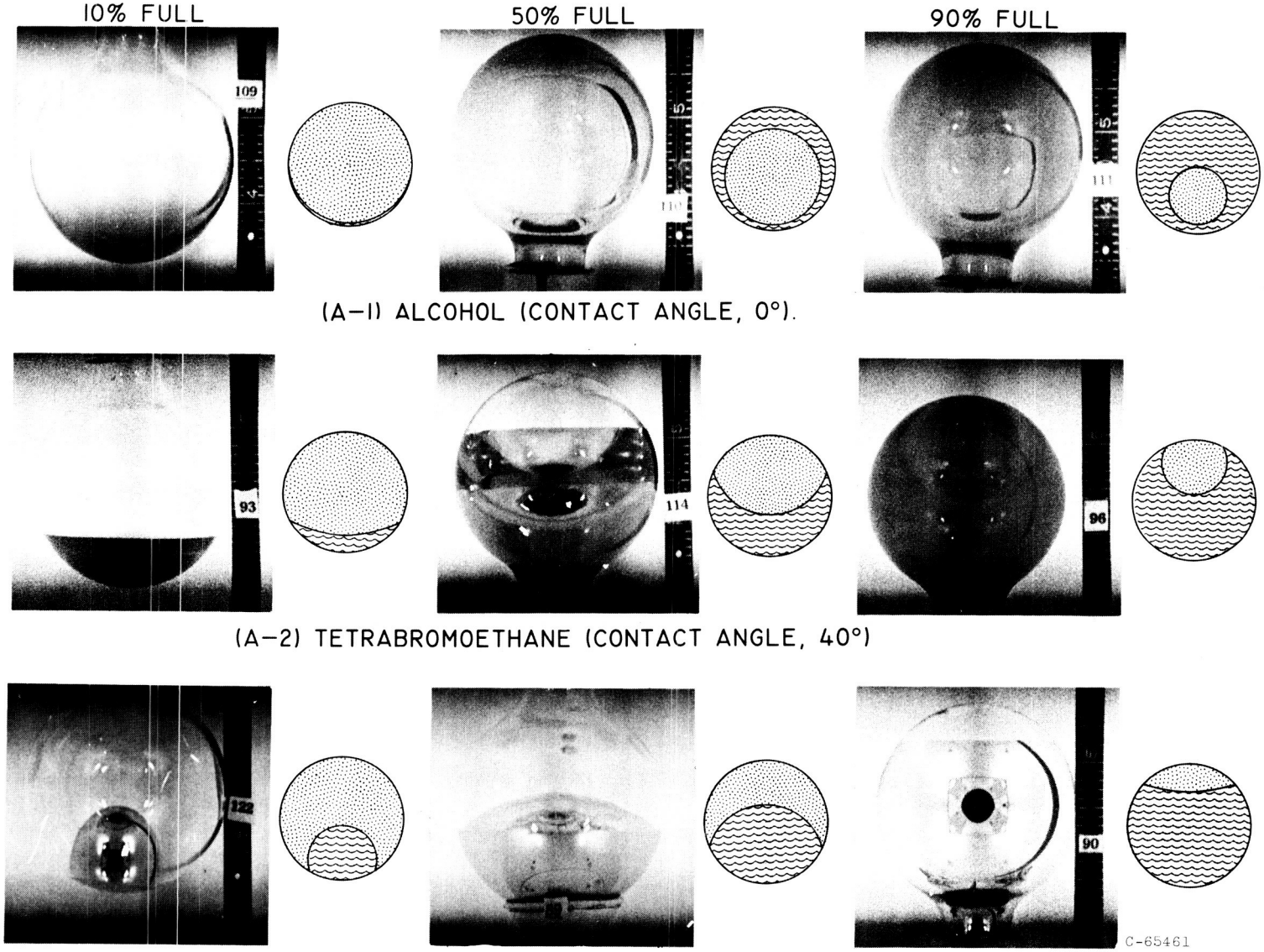


(a) In spheres.

Figure 7. - Configuration of liquid-vapor interface during weightlessness.

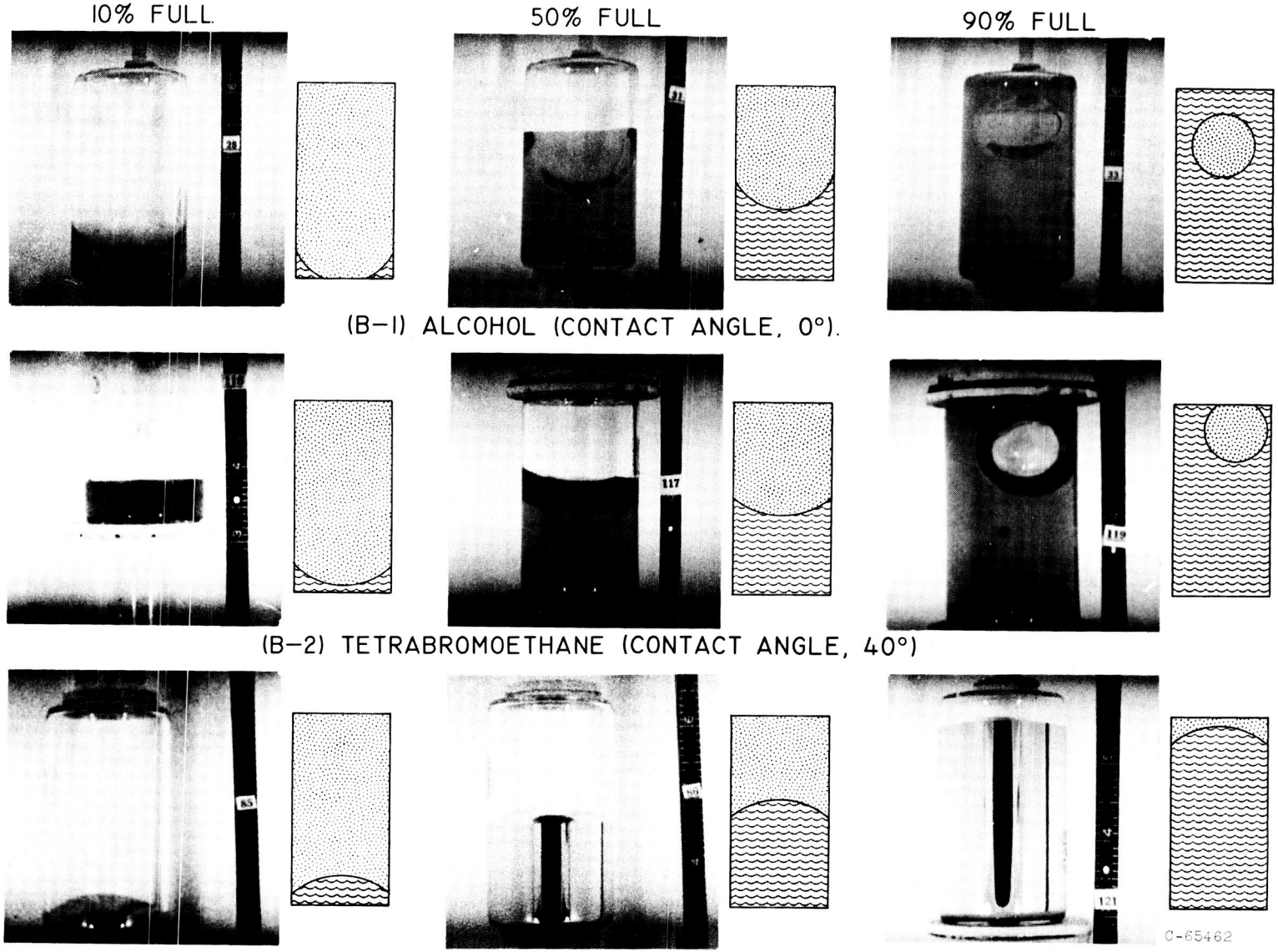


(b) In cylinders.

Figure 7. - Continued. Configuration of liquid-vapor interface during weightlessness.

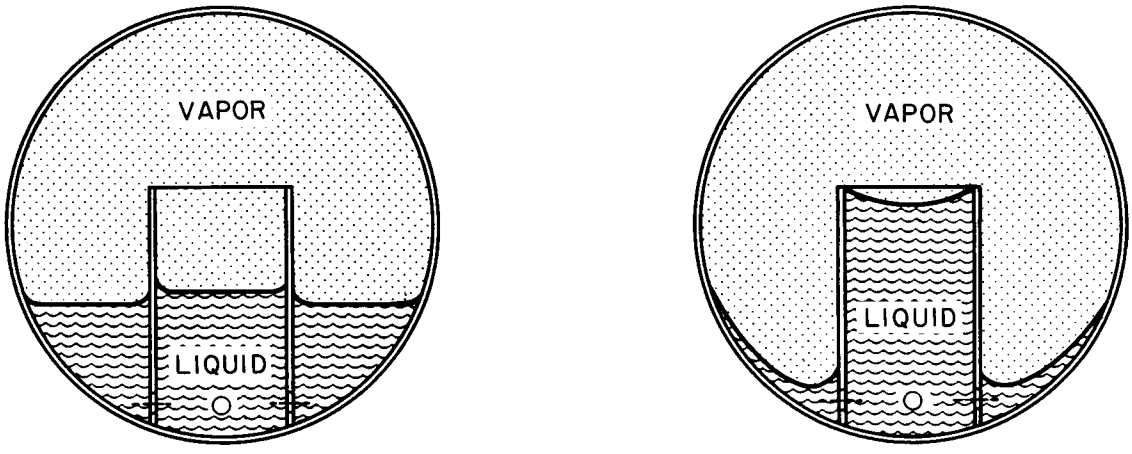


(a) 1-g configuration.

(b) Zero-g configuration.

Figure 8. - Capillary-type ullage control surface.

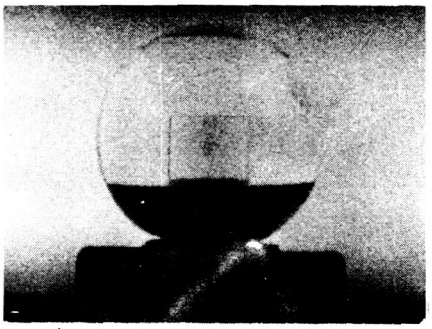

1-G CONFIGURATION

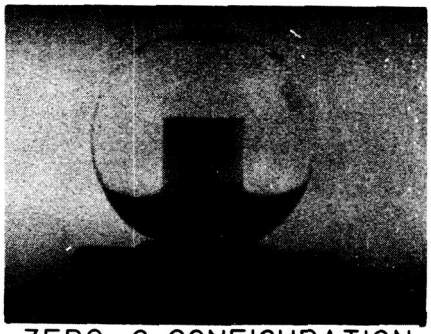

ZERO-G CONFIGURATION

(a) Initial mounting angle, $0^{o}$.

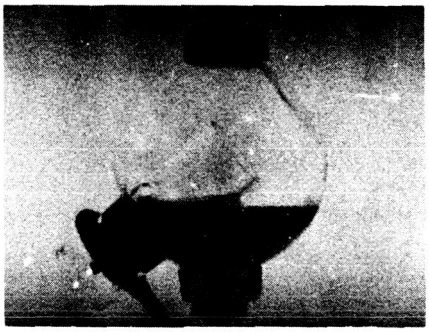

1-G CONFIGURATION

ZERO-G CONFIGURATION

(b) Initial mounting angle, $45^{o}$.

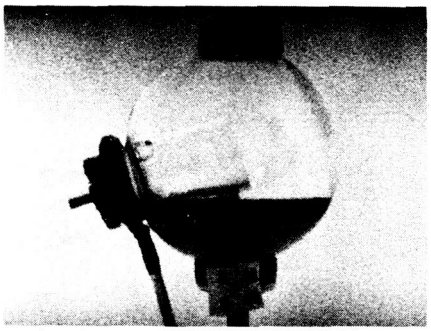

1-G CONFIGURATION

ZERO-G CONFIGURATION

(c) Initial mounting angle, $75^{o}$.

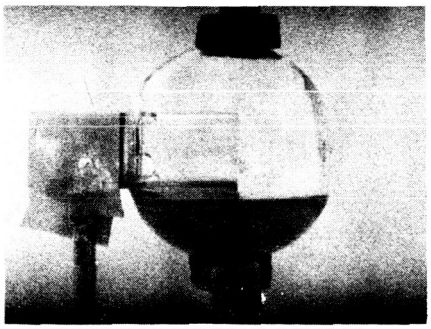

1-G CONFIGURATION


APPROACHING STEADY-STATE
ZERO-G CONFIGURATION

(d) Initial mounting angle, $90^{o}$.

Figure 9. - Photographs from preliminary drop-tower tests for range on initial mounting angles.

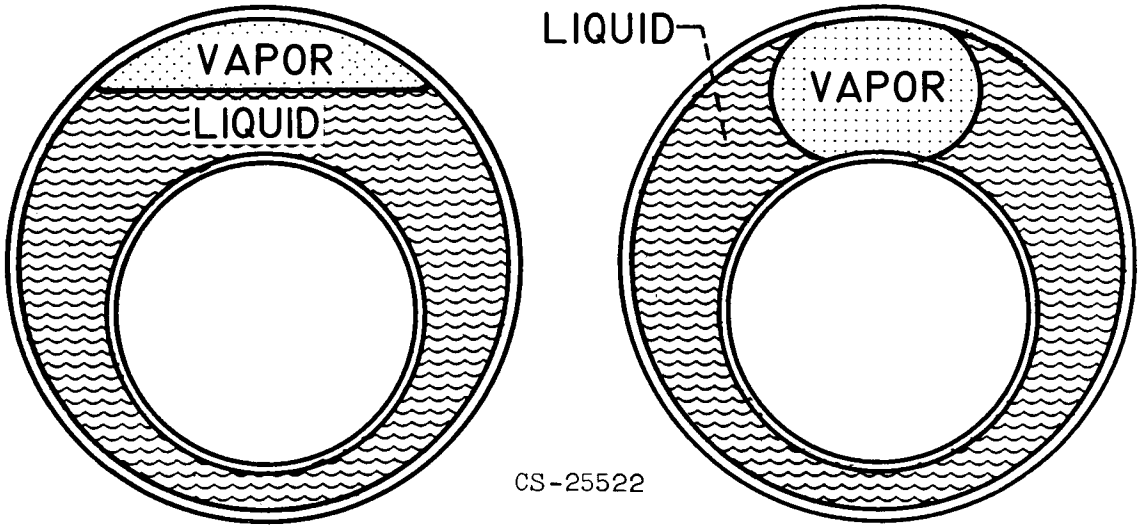


(a) 1-g configuration. (b) zero-g configuration.

Figure 10. - Application of tapered section principle to spherical tank.

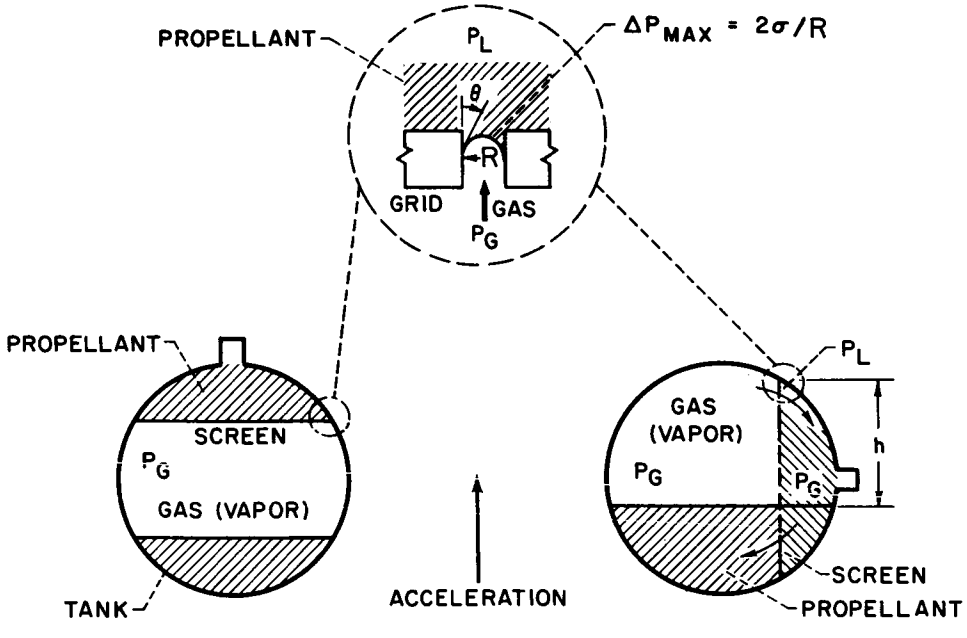


(a) Normal acceleration. (b) Transverse acceleration.

Figure II. - Effect of acceleration on liquid retention power of screens.

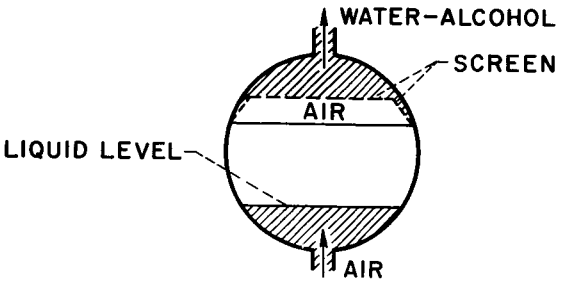


(a) Pie-pan configuration.

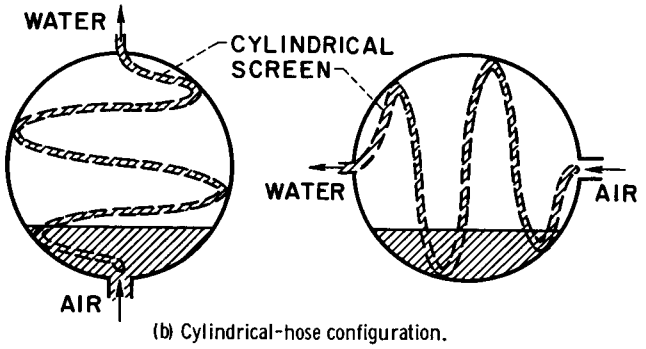


(b) Cylindrical-hose configuration.

Figure 12. - Application of screens to retention of liquid over pump inlet.

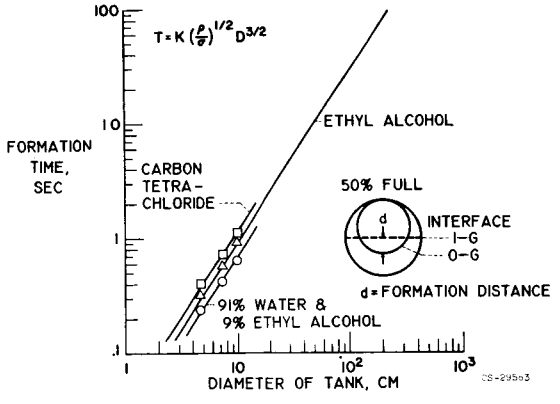


(a) Effect of tank size.

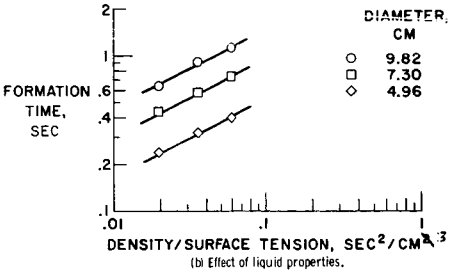


(b) Effect of liquid properties.

Figure 13. - Effect of tank size and liquid properties on interface formation time in spheres after entering zero gravity.

E-2345

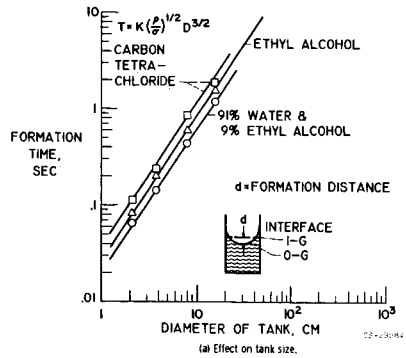


(a) Effect on tank size.

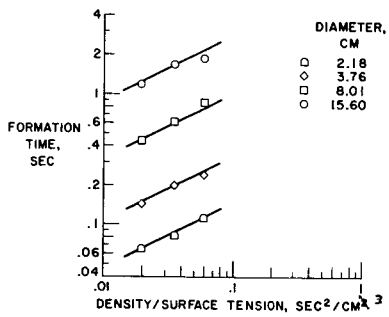


(b) Effect of liquid properties.

Figure 14. - Effect of tank size and liquid properties on interface formation time in cylinders after entering zero gravity.

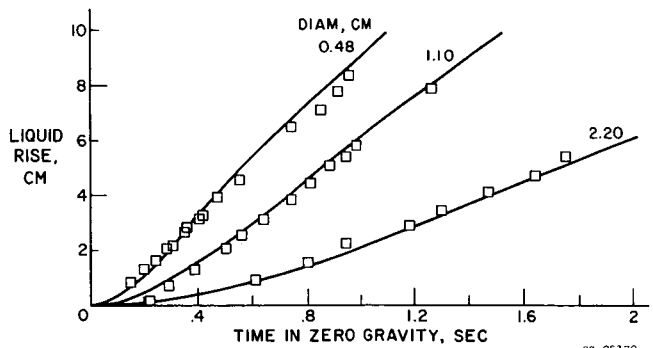


(a) Comparison of analytical and experimental results.

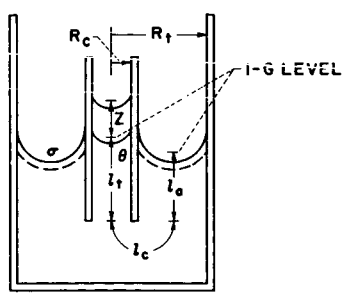


(b) Geometry and nomenclature of capillary system.

Figure 15. - Variation of liquid rise in a capillary tube with time in zero gravity.

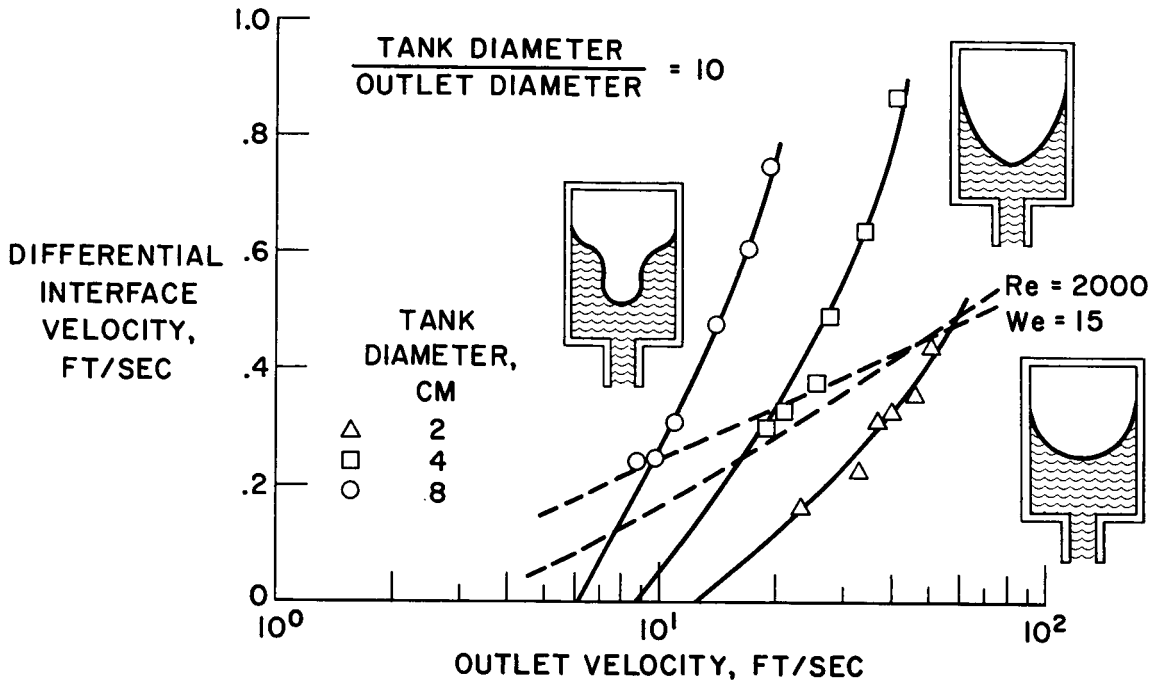


Figure 16. - Effect of outlet velocity on interface distortion.

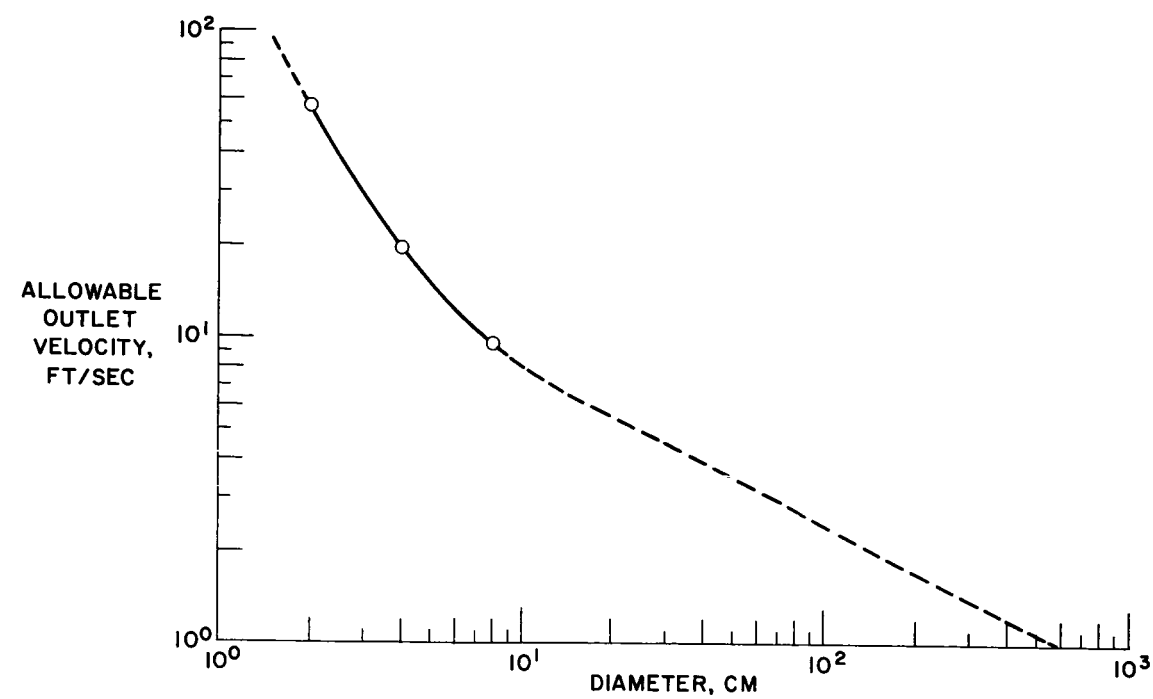


Figure 17. - Allowable outlet velocity as function of tank diameter.

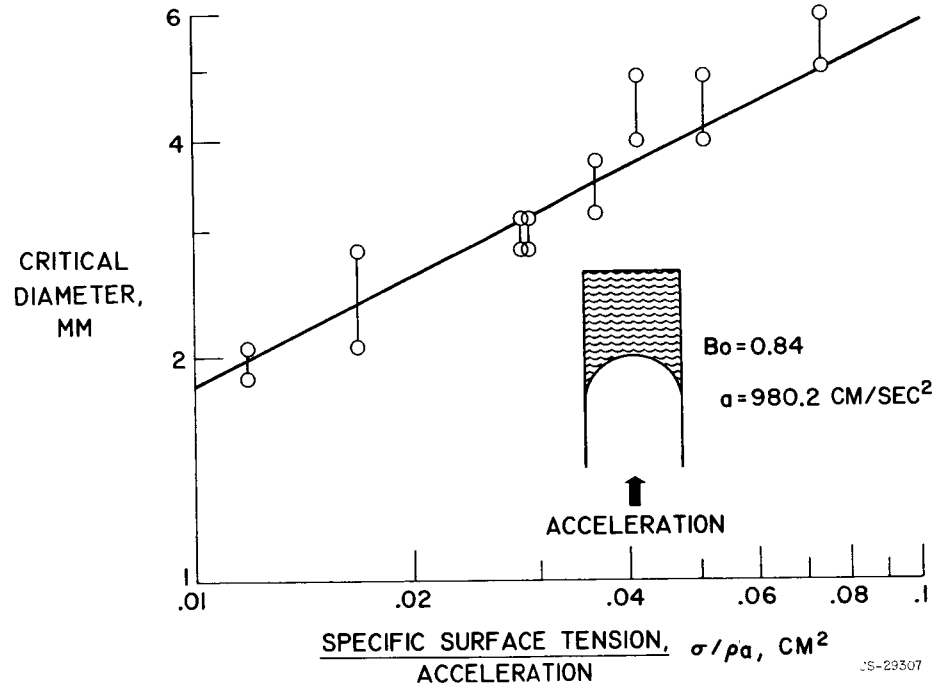


Figure 18. - Stability characteristics in a vertical cylinder.

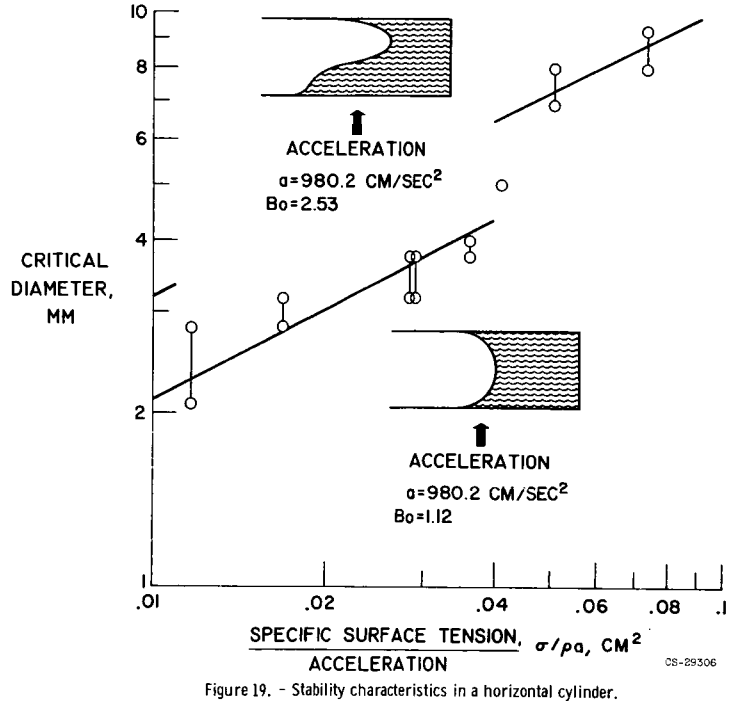


Figure 19. - Stability characteristics in a horizontal cylinder.

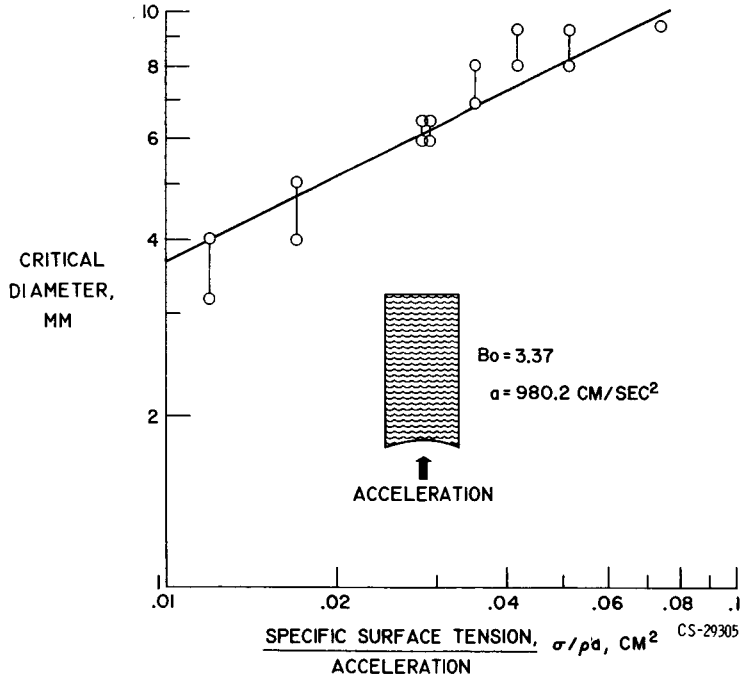


Figure 20. - Stability characteristics at ground edge of a vertical cylinder.

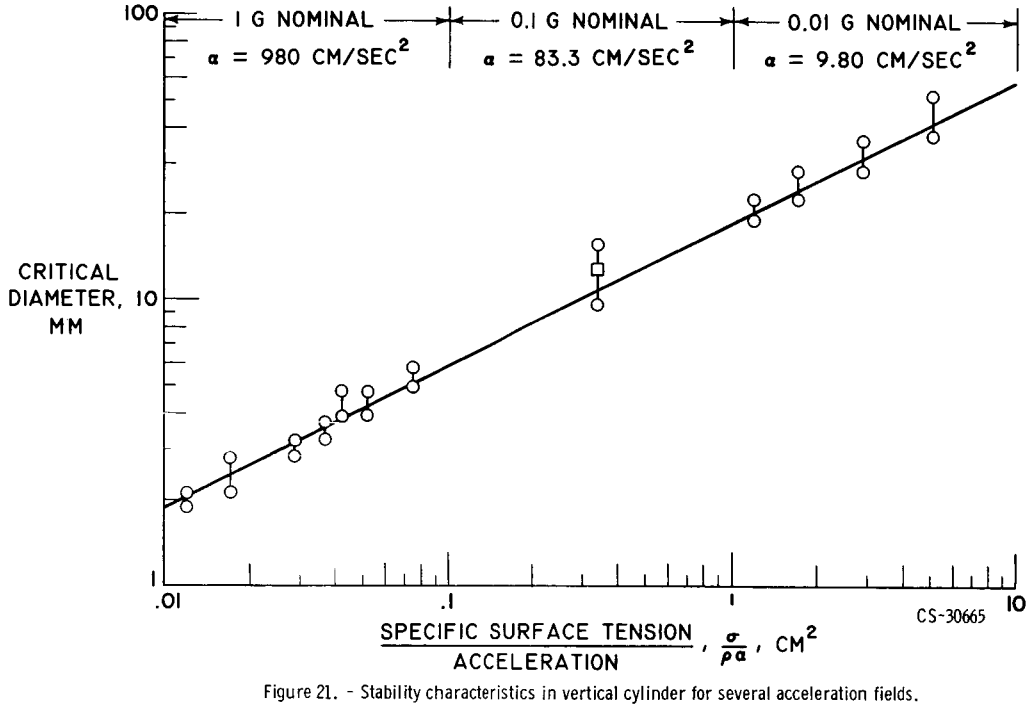


Figure 21. - Stability characteristics in vertical cylinder for several acceleration fields.

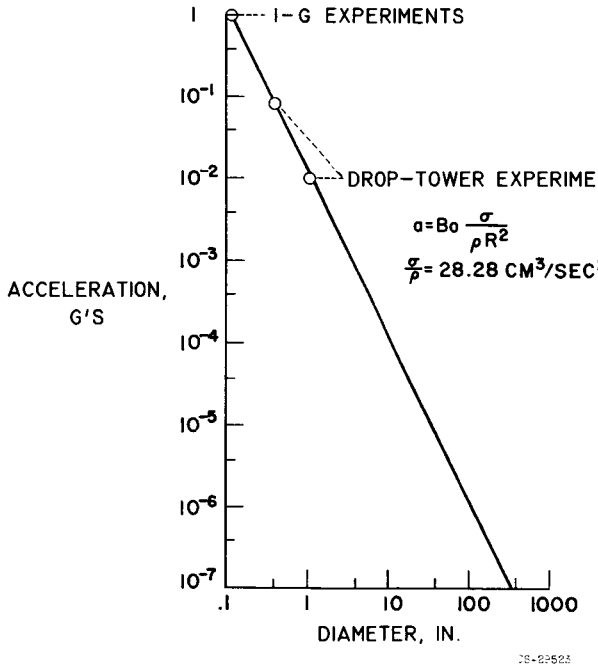


Figure 22. - Interfacial stability as function of acceleration.

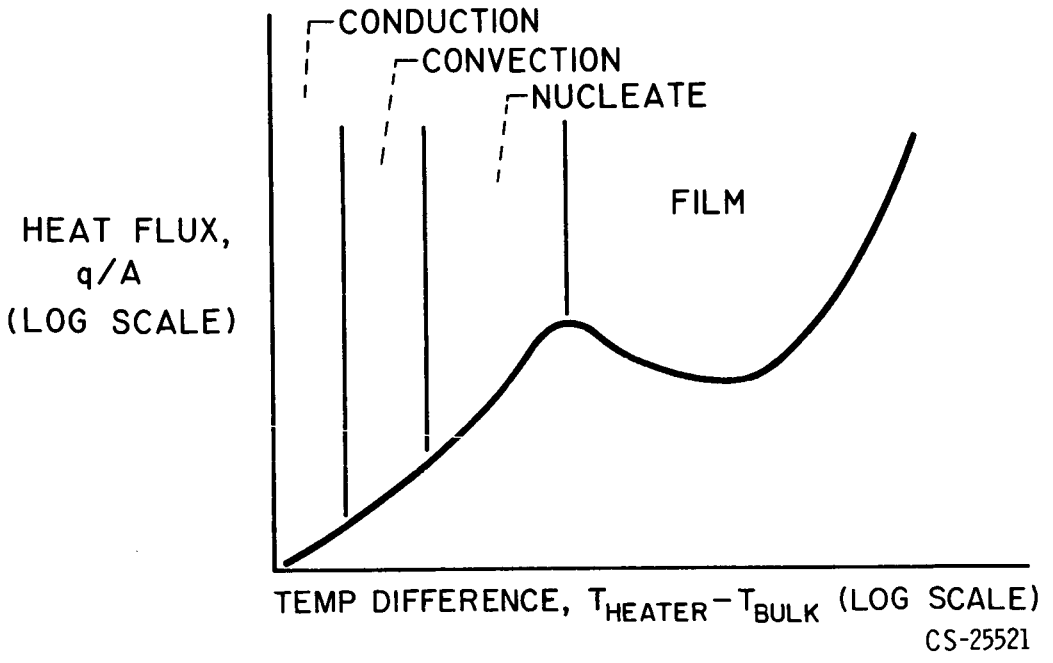


Figure 23. - Typical pool boiling characteristics for 1-g field.

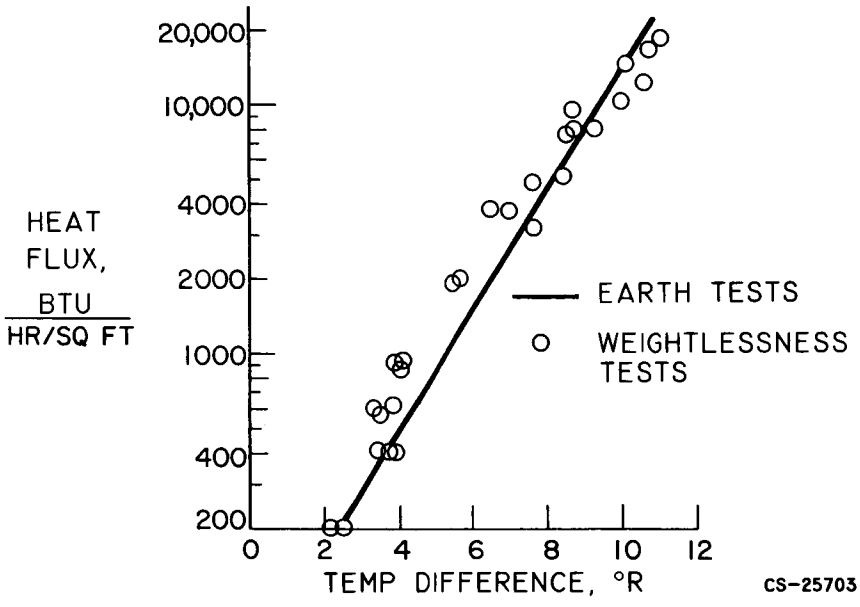


Figure 24. - Comparison of 1-g and zero-g liquid-hydrogen heat-transfer characteristics for nucleate boiling range.

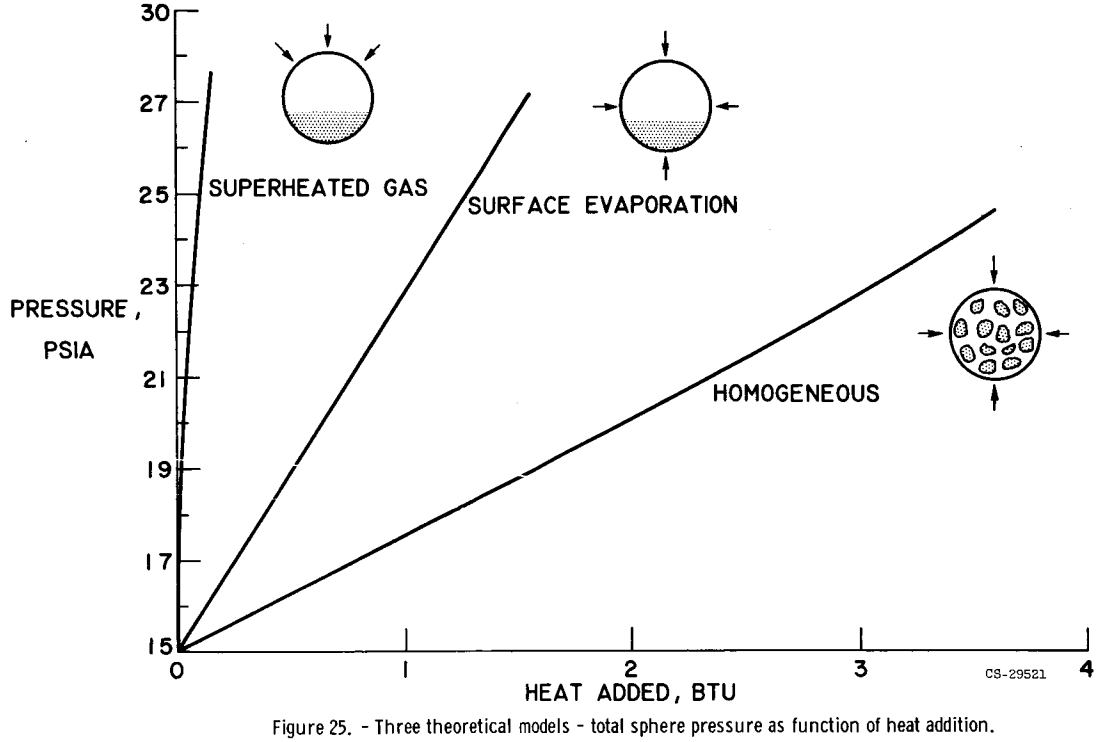


Figure 25. - Three theoretical models - total sphere pressure as function of heat addition.